REPORT DOCUMENTATION PAGE

Form Approved
OMB No. 0704-0188

1a REPORT SECURITY CLASSIFICATION	1b. RESTRICTIVE MARKINGS
UNCLASSIFIED	

2a. SECURITY CLASSIFICATION AUTHORITY	3. DISTRIBUTION/AVAILABILITY OF REPORT
2b. DECLASSIFICATION/DOWNGRADING SCHEDULE	Approved for public release; distribution unlimited.

4 PERFORMING ORGANIZATION REPORT NUMBER(S)	5. MONITORING ORGANIZATION REPORT NUMBER(S)
NRL Memorandum Report 6094	

6a. NAME OF PERFORMING ORGANIZATION	6b OFFICE SYMBOL *(If applicable)*	7a. NAME OF MONITORING ORGANIZATION
Naval Research Laboratory	Code 4420	

6c. ADDRESS *(City, State, and ZIP Code)*	7b. ADDRESS *(City, State, and ZIP Code)*
Washington, DC 20375-5000	

8a. NAME OF FUNDING/SPONSORING ORGANIZATION	8b. OFFICE SYMBOL *(If applicable)*	9 PROCUREMENT INSTRUMENT IDENTIFICATION NUMBER
Office of Naval Research	Code 121	

8c. ADDRESS *(City, State, and ZIP Code)*	10. SOURCE OF FUNDING NUMBERS			
Arlington, VA 22217	PROGRAM ELEMENT NO. 61153N	PROJECT NO. BR021- 01-W1	TASK NO.	WORK UNIT ACCESSION NO.

11. TITLE *(Include Security Classification)*

Ocean and Ship Wave Modification by a Surface Wake Flow Pattern

12. PERSONAL AUTHOR(S)

Griffin, O.M., Keramidas, G.A., Swean, T.F., Jr. and Wang, H.T.

13a. TYPE OF REPORT	13b TIME COVERED	14 DATE OF REPORT *(Year, Month, Day)*	15 PAGE COUNT
Interim	FROM 10/86 TO 3/88	1988 August 1	66

16 SUPPLEMENTARY NOTATION

17	COSATI CODES		18. SUBJECT TERMS *(Continue on reverse if necessary and identify by block number)*	
FIELD	GROUP	SUB-GROUP	Ocean waves	Wake
			Wake detection	Ship waves
			Marine hydrodynamics	

19 ABSTRACT *(Continue on reverse if necessary and identify by block number)*

Ocean surface waves are altered by interactions with mean and fluctuating surface currents. These waves may be ambient or ship-generated, or may be a combined system produced by both sources of generation. An important wave-current interaction is caused by the interaction of the waves with the surface wake produced by the passage of a surface ship. Remote observations of a ship wake using synthetic aperture radar (SAR) show distinct features such as a dark trailing centerline region and bright-line images aligned at some angle to the ship's path. The dark region of relatively low radar backscatter is usually associated with a "dead water" region which is relatively devoid of short wave components, while the bright line feature suggests a region of enhanced radar return within the apparent angular confines of the ship's Kelvin wave pattern.

(Continues)

20 DISTRIBUTION/AVAILABILITY OF ABSTRACT	21. ABSTRACT SECURITY CLASSIFICATION
☒ UNCLASSIFIED/UNLIMITED ☐ SAME AS RPT ☐ DTIC USERS	UNCLASSIFIED

22a. NAME OF RESPONSIBLE INDIVIDUAL	22b. TELEPHONE *(Include Area Code)*	22c OFFICE SYMBOL
Owen M. Griffin	(202) 767-2904	Code 4420

DD Form 1473, JUN 86   *Previous editions are obsolete.*   SECURITY CLASSIFICATION OF THIS PAGE

S/N 0102-LF-014-6603

19. ABSTRACTS (Continued)

    In this report the interactions of ship-generated Kelvin waves and ambient waves with the momentum wake of a surface vessel are studied to assess the effectiveness of the momentum wake in the generation of these remotely-observed features. Other factors such as the limiting wave steepness at the onset of wave breaking also are considered.

CONTENTS

Naval Research Laboratory

Washington, DC 20375-5000

Ocean and Ship Wave Modification by a Surface Wake Flow Pattern

O. M. GRIFFIN, G. A. KERAMIDAS, T. F. SWEAN JR., AND H. T. WANG

*Laboratory for Computational Physics
and Fluid Dynamics*

August 4, 1988

OCEAN AND SHIP WAVE MODIFICATION
BY A SURFACE WAKE FLOW PATTERN

INTRODUCTION

Ocean surface waves are altered by interactions with mean and fluctuating surface currents. These waves may be ambient or ship-generated, or may be a combined system produced by both sources of generation. An important wave-current interaction is caused by the interaction of the waves with the surface wake produced by the passage of a surface ship. Remote observations of a ship wake using synthetic aperture radar (SAR) show distinct features such as a dark trailing center-line region and bright-line images aligned at some angle to the ship's path. The dark region of relatively low radar backscatter is usually associated with a ''dead water'' region which is relatively devoid of short wave components, while the bright line feature suggests a region of enhanced radar return within the apparent angular confines of the ship's Kelvin wave pattern.

In this report the interactions of ship-generated Kelvin waves and ambient waves with the momentum wake of a surface vessel are studied to assess the effectiveness of the momentum wake in the generation of these remotely-observed features. Other factors such as the limiting wave steepness at the onset of wave breaking also are considered.

A subsequent section of this report will briefly survey related hydrodynamic studies which are available in the literature. A fundamental point from all of these studies is the importance of the wave action, or the energy divided by the wave intrinsic frequency, as the appropriate conserved quantity for wave motions in the presence of surface currents. It is the wave action, and not the wave energy, which must be considered when surface gravity waves are modified by their interactions with currents. The basic theory to be described will show that the interaction between the waves and the ship wake is described by characteristic equations for the kinematics and the conservation of wave action spectral density for continuous spectra, defined as the energy per unit frequency. Solution of these equations gives the changes in the paths of the waves propagating through the ship wake, the changes in their wavenumbers, and the changes in the amplitudes of the spectral components.

The results of application of the theory include predictions of Kelvin waves for a high-speed destroyer, ambient wave modifications, ship wave modifications, and a brief comparison with experiments. The modification of an ambient wave field by a surface current pattern is demonstrated by the spatial variation of the spectral composition and the surface displacement of the wave pattern. The effects of wave reflection, refraction and breaking are accounted for in the model. It is shown that the near-field centerline region of the ship wake is remarkably free of short wave components, but the downstream extent of this region is not sufficient to explain the long distances over which the dark stem region of radar return persists. The turbulent wake of a ship alters the Kelvin wave pattern generated by the ship's passage. This interaction leads directly to a narrower than usual wedge-shaped region within which the divergent waves are dominant. The angular directions of these waves are shifted so that they travel at angles more nearly normal to the ship track. The lengths of the waves also are reduced, which may cause them to steepen.

SAR IMAGERY OF SHIP WAKES

One of the striking features of the remote observation of surface ship wakes using synthetic aperture radar (SAR) imagery is the apparent variability of the wake angles. The usual Kelvin wave pattern generated by the steady motion of a ship is included within an angular region between ± 19.5 degrees from the ship track. However, many of the SEASAT satellite-based SAR images produced wake half-angles in the ranges from 14 to 17 degrees and as small as 1 to 7 degrees. A typical example of a SAR image of a surface ship wake is shown in Fig. 1.

A program of sea trials was conducted jointly by the Naval Ocean Systems Center (NOSC) and the Canadian Defense Research Establishment Pacific (DREP) to determine the detectability of wakes by SAR ocean wave pattern imaging (Hammond et al., 1985). Ship-generated waves of known wavelength and direction were observed with an airborne L-band SAR to study, under selected sea conditions, the hydrodynamic contributions to the detectability of the wake. The results of the study led to the initial conclusion that the narrow-v angles of the ship wave pattern were produced by an interaction between the ship-generated waves and longer waves present in the test area. Lyden et al. (1985) analyzed much of the narrow-v wake data from these experiments and concluded that the bright images were produced by ship-generated Bragg waves moving away from the ship track. There were only light winds at the field test site during these experiments.

A review of the available synthetic aperture radar images of the narrow-v wakes available through mid-1985 was made by Witting and Vaglio-Laurin (1985). Among the images discussed were those taken from SEASAT and the airborne SAR images obtained during the DREP experiments. A proposed mechanism for the generation of the narrow-v wakes was based upon the development of turbulent eddies with length scales on the order of the Bragg wavelength in the boundary layer and near wake regions of the ship. Wave breaking also was thought to play an important role in enhancing the radar image of the wake. No actual predictions of the observed wake configurations were made as part of the study.

It has been concluded by Munk et al. (1987) that the SAR images of the narrow-v wakes are caused by intermittency or unsteadiness in the divergent waves of the Kelvin wake producing wavelengths in the Bragg scattering range of the radar. This generally supports the previous hypothesis of Lyden et al. (1985). High resolution photographs of ship wakes taken during a 1985 Shuttle mission also were analyzed by Munk et al. In contrast to the radar images it was concluded that the optical images were due to interference fringes resulting from a complex geometry of sources in the ship wake. Low wind conditions prevailed in the vicinity of the wake detection and observation.

The most recent remote observations of v wake patterns were made during a series of experiments conducted with the Shuttle Imaging Radar-B (SIR-B) during a mission of the space shuttle Challenger in October 1984 (A.M. Reed, 1986). The SAR was an L-band instrument which was deployed during several orbits of the shuttle to record the radar images of surface ship wakes. No narrow-v wakes with half-angles of 1 to 7 degrees were observed. Rather, the half-angles of the v wake patterns were clustered, with some variability, in the range of 14 to 16 degrees. All of the v wakes were observed when the ships were moving in the azimuthal direction or at 45 degrees to azimuth relative to the shuttle orbit direction. In all of these experiments the azimuthal direction of ship movement was parallel to the shuttle direction.

In contrast to the bright v wake images which are often observed using synthetic aperture radar, there also is a relatively narrow, stem-like dark image along the ship track which commonly persists for many kilometers downstream. The dark portion of the radar image suggests that this region of the

2
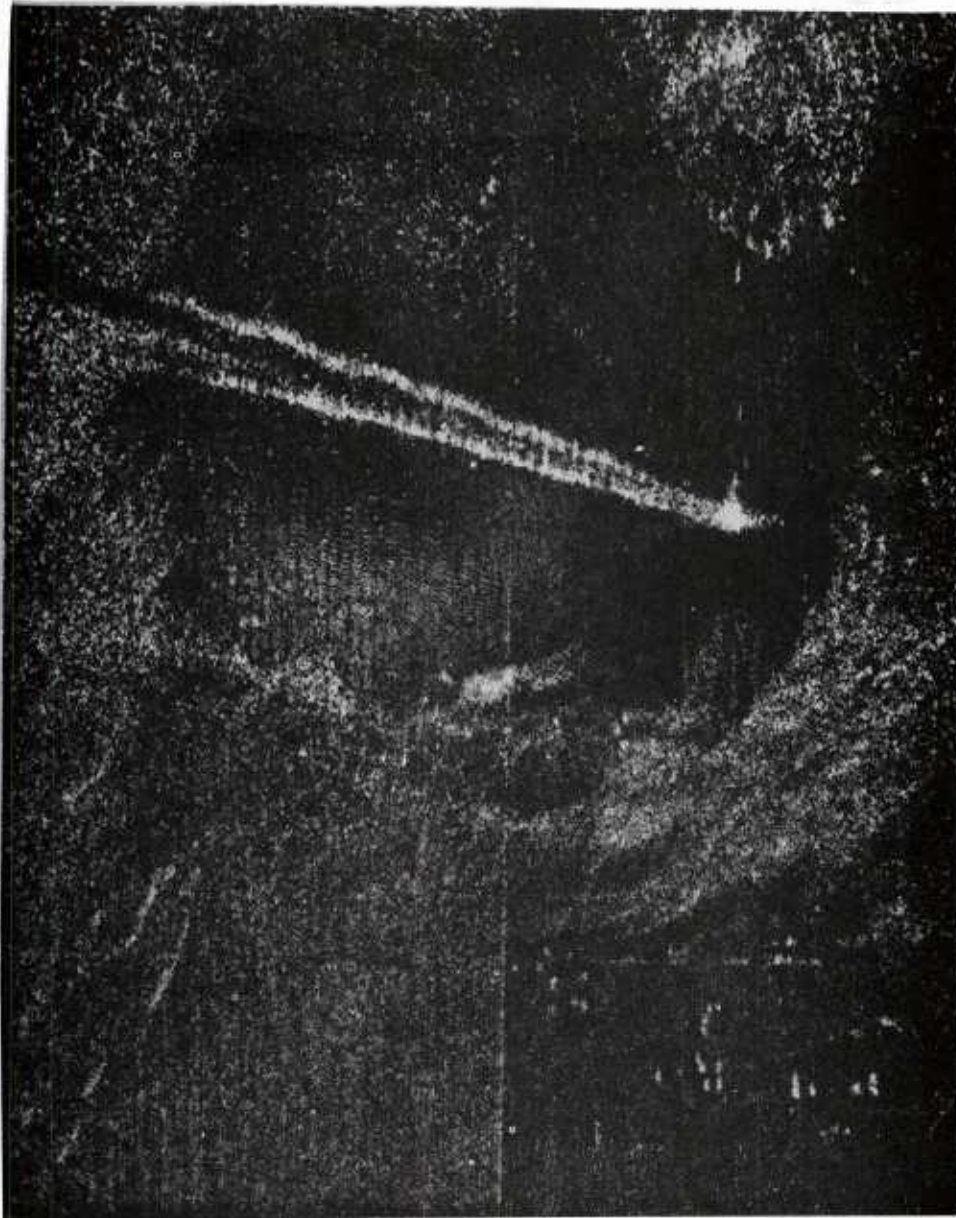
Fig. 1 — A digital ground range SAR image of the narrow-v wake of the USS QUAPAW during the 1983 Georgia Strait experiments; from Lyden et al. (1985).

surface is relatively smooth and free of short-wavelength scatterers. This region has been described as the turbulent wake or scar of the ship, but the recent computations by Swean (1987) to simulate the wake of a twin-screw high speed destroyer from model test data suggest strongly that the surface features of the classical turbulent ship wake do not persist sufficiently far downstream to explain the SAR images. These computations are summarized in a later section of this report. Another suggestion based upon the results of a recent NRL field experiment is that the persistence of the dark scar region is due to the redistribution of surfactant materials at and near the water surface as a result of the ship's passage (Kaiser et al., 1987).

RELATED HYDRODYNAMIC STUDIES

Among the earliest and most comprehensive studies of the interaction between linear surface waves and currents is the work of Longuet-Higgins and Stewart (1961, 1964). Because of the assumptions inherent in these studies, they were limited to the propagation of short waves. Thus the characteristic length of the wave train is much less than the length scale of the flow field over which it progresses. Peregrine (1971) studied the interaction between a ship's wake and its wave system using a formulation based upon the work of Longuet-Higgins and Stewart. Except for very weak surface wakes the included half-angle of the wave pattern was found to be less than that of the well-known Kelvin ship wave pattern (Ursell, 1960). Under certain limiting conditions the radiated steady ship waves at infinity depend only on the maximum value of the surface current in the wake.

More recently, Peregrine and Thomas (1979) have considered the same problem for finite-amplitude, symmetric waves. This approach is based upon the conservation of wave action as discussed by Lighthill (1979) and Crapper (1984), and in the related work of James et al. (1977), Cooper and Griffin (1986), and Cooper, Griffin and Wang (1987). The finite-amplitude wave properties were computed by Peregrine and Thomas using the method of Longuet-Higgins (1975) for predicting the energy and wave action densities and fluxes. These studies show that it is the wave action and not the wave energy which should be considered when the gravity wave field is modified by its interaction with a surface flow field.

Savitsky (1970) conducted an experimental study of the interaction between deep water gravity waves and a near-surface turbulent flow field. The flow consisted of mean and random turbulent wake components which were generated by the steady motion of a grid in the same direction as the wave motion. The presence of the mean velocity gradients in and near the surface plane resulted in wave refraction, diffraction and interference effects which reduced the wave heights in the wake region to approximately 10 percent of their original value. Outside of the wake the resultant local wave heights were increased by as much as 75 percent above their original values.

Studies of irregular or random wave field interactions as considered here were conducted by numerous workers, e.g. Karlsson (1969), Tayfun et al. (1976), James et al. (1977), Sakai et al. (1983), and Hedges et al. (1985). The results of Tayfun et al. and James et al. are most relevant here as they form the basis for the work to be outlined in this report. For more complete details of the model, the reader is referred to Cooper (1986). The mathematical foundations for the overall approach taken here are discussed by Skop (1984).

MODEL TEST DATA

The model test data employed in this study were obtained from towing basin tests of a twin-screw high speed destroyer model (Lindenmuth, 1986). The model and test conditions as they relate to the present study are summarized in Table 1. Mean velocities, rms turbulence velocities, and the Reynolds stresses were obtained at several planes aft of the model using a laser-Doppler anemometer (LDA) and a hot-film anemometer array.

Table 1 — Twin-Screw High Speed
Destroyer Ship Parameters (1/25 scale)

Model DTNSRDC No.	High Speed Destroyer 5415-01
Length* Beam Draft Prop Dia. Block Coef.	18.8 *ft* 29.9 *in* 9.8 *in* 8.16 *in* 0.506
Tow Speed Froude No.	4.0 *knots* 0.28

*Length between forward and aft perpendiculars.

These data subsequently were employed in a numerical simulation of the downstream evolution of the model's turbulent wake (Swean, 1987). The initial plane of the calculation was located four ship beams downstream of the stern of the model. A contour plot in the y-z plane of the downstream (x-direction) mean velocity at this location is shown in Fig. 2, for the experiments with outboard propellor rotation. These data represent an interpolation of the experimental data directly to the computational grid. The calculation extended downstream to approximately twelve ship beams aft. The velocities in the initial plane at three typical depths below the free surface are plotted in Fig. 3. The velocity here is measured relative to still water, so that

$$\frac{\Delta u}{U} = \frac{\overline{U}(y, z)}{U} - 1 \tag{1}$$

where U is the ship velocity (tow speed). The negative values of Δu are in the direction of the ship motion and are representative of a drag wake. As the depth increases, there is a change of sign and Δu becomes positive due to the propellor thrust.

A contour plot of the surface (x-y) plane distribution of mean velocity Δu in the x direction is shown in Fig. 4a, where the downstream and cross-stream distances are scaled by the ship beam B. The computed results show that the mean surface features of the wake are greatly diminished at x / B = 12, the downstream limit of the experimental domain. This distance corresponds to approximately 1.6 ship lengths, so it is clear that the free surface mean velocity field in the wake of a ship has greatly diminished after but a few ship lengths aft of the vessel. The calculation recently has been extended to 1000 ship beams downstream, and the results are shown in Fig. 4b. In the far wake the propellor thrust has broached the surface and has displaced the drag wake outboard.

An estimate of the width of the early turbulent wake at the surface can be made from the results of the calculation. If the contour of

$$\left| \frac{\Delta u}{U} \right| = 0.01, \tag{2}$$
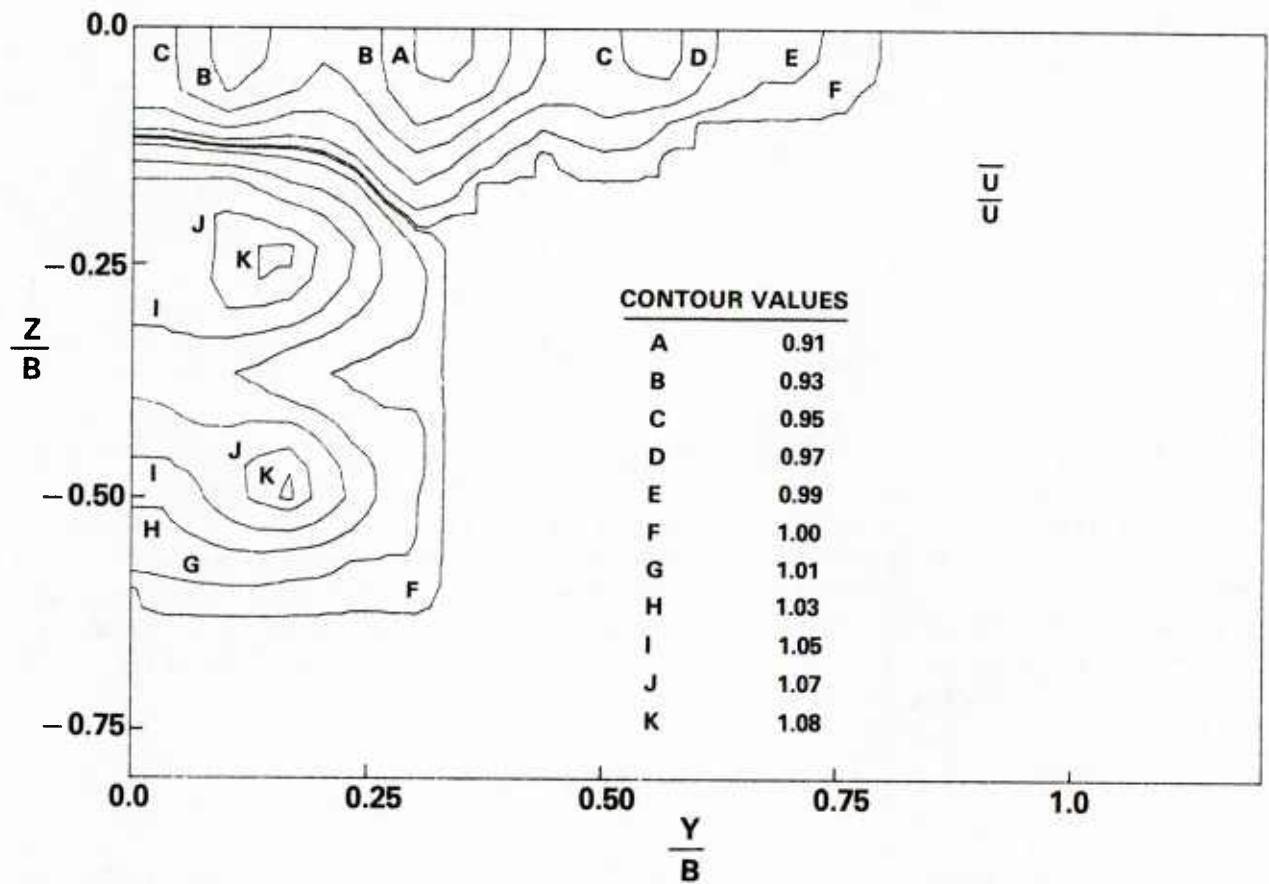
Fig. 2 — The initial $(y - z)$ mean velocity plane for the calculation of the turbulent wake of the Model 5415 high speed destroyer model.
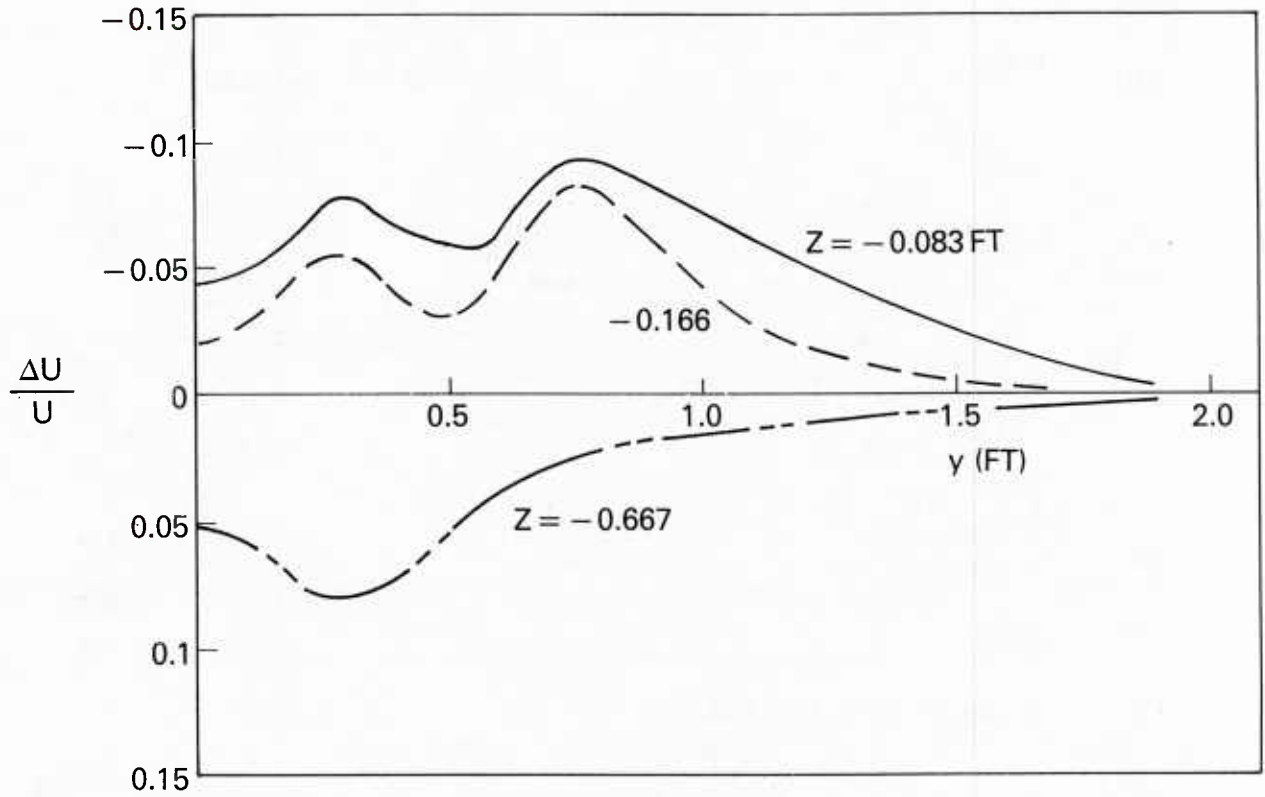
Fig. 3 — Measured mean velocities $\Delta u / U$ at three typical depths in the initial $(y - z)$ plane of the Model 5415 wake. (1 ft = 0.305 m)
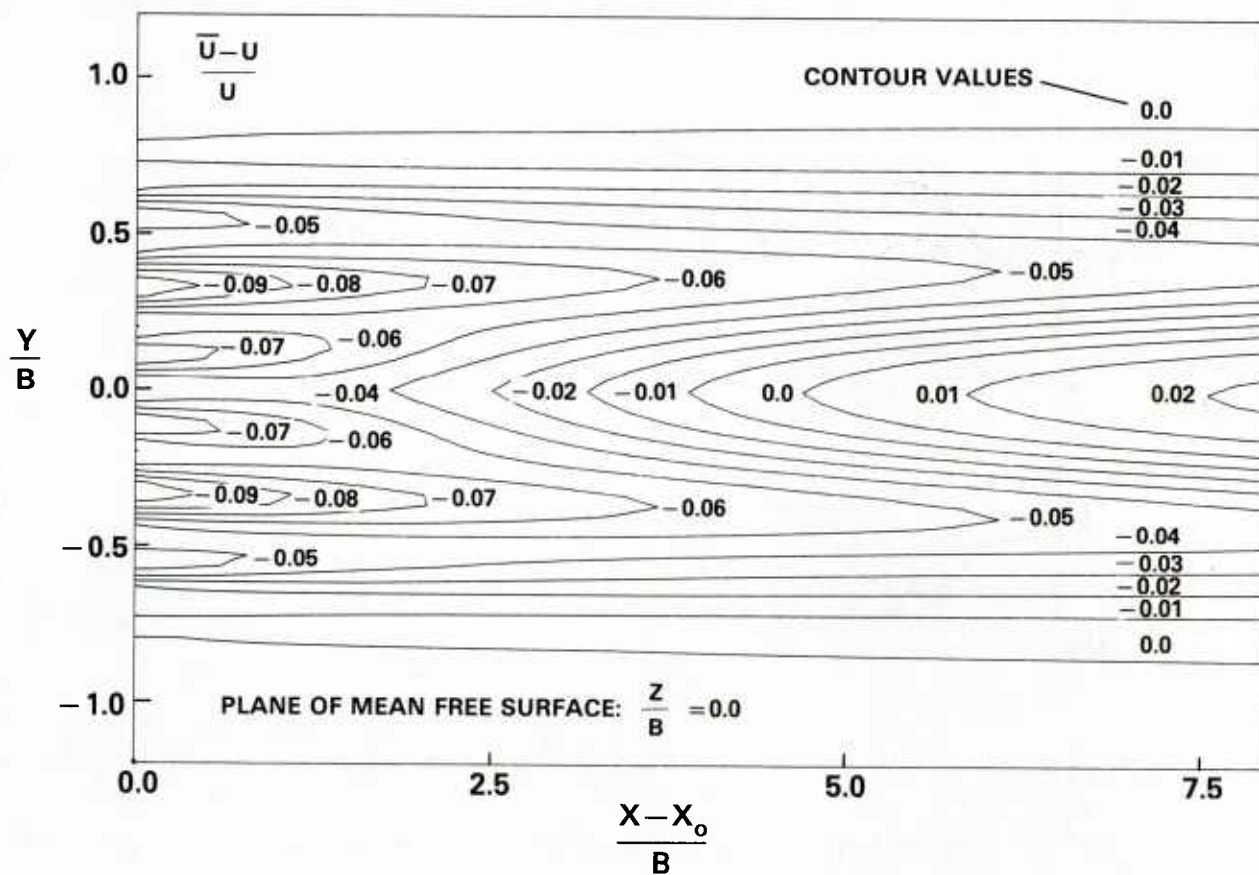
Fig. 4a — Contour plots of the surface (x,y) plane distribution of mean velocity $\Delta u / U$ from the calculation of the Model 5415 wake; from Swean (1987).

The early wake, $0 \le (x - x_0)/B < 12$.
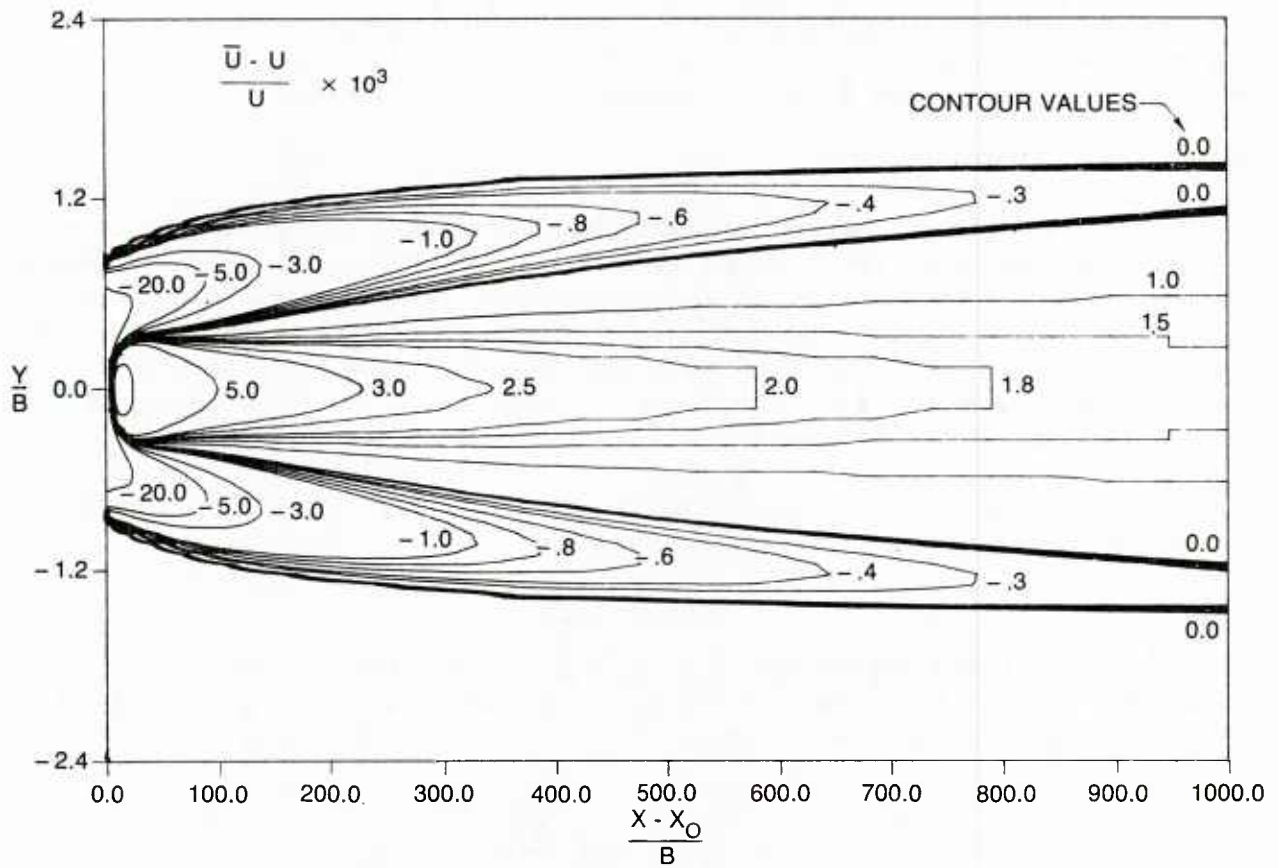
Fig. 4b — Contour plots of the surface (x,y) plane distribution of mean velocity $\Delta u /U$ from the calculation of the Model 5415 wake.

The late wake, $0 \leq (x - x_0)/B < 1000$.

9

which is shown in Fig. 4a, is chosen arbitrarily as the cross-stream limit of the wake, then the half-width d / B ~0.75. This is approximately half of the wake width which typically is measured from aerial photographs of the visible "white water" wake of a surface ship (Peltzer, 1984). A comparable representation of the wake half-width d at 500 ship beams (500 B) downstream in Fig. 4b is d/B = 1.25 when the $\Delta u = 0$ contour is employed there to define the cross-track extent of the surface wake. This is equivalent to 66 ship lengths for the destroyer model with B/L = 0.133. A typical example of the visible white water wake from the study by Peltzer is shown in Fig. 5. The visible white water far wake at the surface usually spreads as shown at an angle of 1 to 1 1/2 degrees, downstream from the initial spreading region directly adjacent to the stern of the ship.

OCEAN WAVE MODIFICATIONS

Relative to a body fixed frame, the far-field surface wake produced by a moving vessel is steady and can be approximated as a parallel shear $u(y)$. Here u is the velocity component in the direction of ship motion, x, and y is the transverse horizontal coordinate. Velocity gradients in the y-direction are assumed to be much greater than those in the x-direction. Variations in the x direction are assumed to be extremely slow. For surface waves interacting with a steady parallel shear current, the total or extrinsic frequency, ω, and the component of wave number in the x direction, k_x, are conserved (James et al., 1977). The random wave field may be characterized by means of the spectral density. To describe the refraction of these waves by the steady surface current, the frequency-direction spectral density is most convenient since the total frequency ω is conserved. The frequency-direction spectral density $\Phi(\omega, \theta ; x)$ is defined from

$$d\tilde{E} = \Phi(\omega,\theta;\mathbf{x})\omega d\omega d\theta \tag{3}$$

where $d\tilde{E}$ represents the mean square surface displacement contribution for waves propagating in directions between θ and $\theta + d\theta$ and possessing total frequencies between ω and $\omega + d\omega$. The total energy is obtained by integration over all angles $-\pi \le \theta \le \pi$ and over all frequencies $0 \le \omega < \infty$, yielding

$$<\zeta^2> = \int_\omega \int_\theta \Phi(\omega,\theta;\mathbf{x}) \, \omega d\omega d\theta. \tag{4}$$

It follows that the contribution to surface elevation corresponding to frequencies of $\Delta\omega$ about ω_j, and directions $\Delta\theta$ about θ_i is given by Wang (1985) as

$$\zeta_{ij} = \sqrt{2\Phi(\omega_j,\theta_i,\mathbf{x})\,\omega_j\,\Delta\omega\,\Delta\theta}\; \cdot$$

$$\cos\left\{ k_{ij}\,(x\,\sin\theta_i + y\,\cos\theta_i) - \omega_j\,t + \phi_{ij} \right\} \tag{5}$$

where the wave number k_{ij} corresponding to refracted waves of frequency ω_j traveling in a direction θ_i is determined from the dispersion relation for linear deep water waves as

$$k_{ij} = \frac{\omega_j^2}{g}\left[\frac{\sqrt{1 + 4\Lambda\eta} - 1}{2\Lambda\eta} \right]^2, \tag{6}$$

where

$$\eta = \omega_j^*\sin\theta_i, \quad \omega^* \equiv \omega\,V_m/g\,, \quad \Lambda(y) = u(y)/V_m$$

10
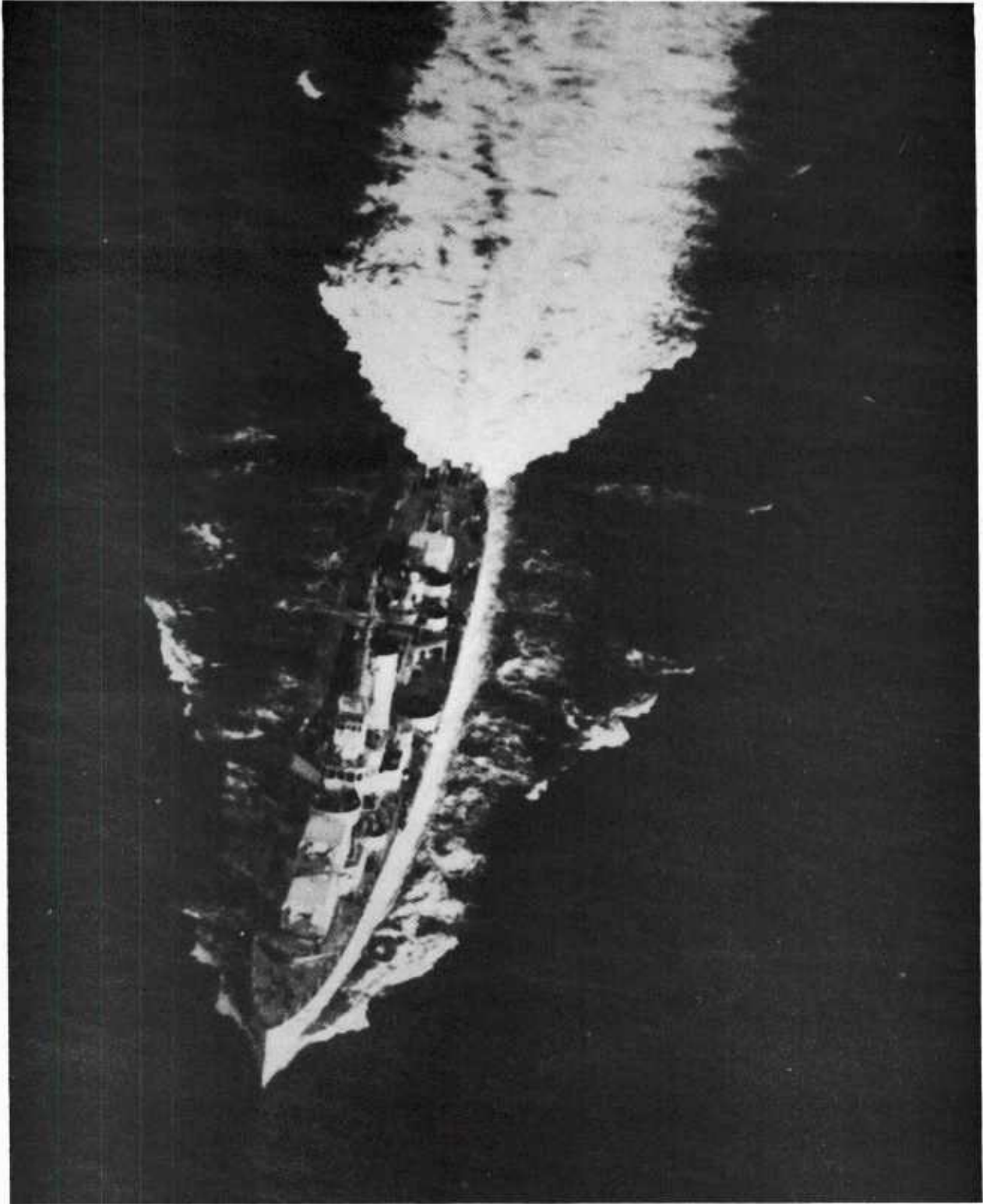
Fig. 5 — A typical aerial view of the white water region behind a surface ship underway; from Peltzer (1984).

and ϕ_{ij} represents a random phase shift uniformly distributed between 0 and 2π. In Eq. (6) V_m represents the maximum value or strength of the surface current distribution, $u(y)$, and g denotes the acceleration of gravity. The full free surface realization or displacement at a given time is represented by the double summation

$$\zeta(x, y) = \sum_i \sum_j \zeta_{ij}(\omega_j, \theta_i; x, y). \tag{7}$$

It is apparent that the major task in characterizing the interaction of the ambient wave field and the surface current $u(y)$ is the evaluation of the modified spectral density Φ. The local value of spectral density is determined from its ratio to the undisturbed value along a ray

$$\Phi = \Phi_\infty \left[\frac{\Phi}{\Phi_\infty} \right] = \Phi_\infty A, \tag{8}$$

where from conservation of wave action density

$$A = \left\{ \frac{\sqrt{1 + 4\Lambda\eta} - 1}{2\Lambda\eta} \right\}^4 \frac{1}{\sqrt{1 + 4\Lambda\eta}}. \tag{9}$$

The mean square surface elevation also can be determined by integrating the spectral density in the initial plane $(\omega_\infty, \theta_\infty)$ after a transformation of variables

$$<\zeta^2> = \int_{\omega_\infty} \int_{\theta_\infty} \Phi_\infty A \, \omega_\infty d\omega_\infty \left[\frac{\partial\theta}{\partial\theta_\infty} \right] d\theta_\infty. \tag{10}$$

Along a ray $\omega_\infty = \omega = $ constant and

$$\sin\theta = \frac{\sin\theta_\infty}{(1 - \Lambda\omega^* \sin\theta_\infty)^2} \tag{11}$$

for the steady current, simple shear $u(y)$ case considered here. For evaluation of Eq. (10), the spectral density ratio $A(\omega_\infty, \theta_\infty) = \dfrac{(1 - \Lambda\eta_\infty)^5}{(1 + \Lambda\eta_\infty)}$. The subscript ∞ denotes the ambient value of a quantity along a ray outside the region of current variation.

The above equations form the basis of a numerical procedure to determine the surface elevation field (realization) and the mean-square surface elevation field. Limits for the integration in $\omega - \theta$ space are required to complete the description. These limits are determined from the conditions of wave breaking and wave reflection which result due to interaction with the surface current pattern.

The wave breaking condition selected by James et al. (1977) and which has been used thus far in the present work represents an extreme condition. The wave breaking boundary is defined by the condition that the local component of the current in the direction of the wave motion is equal but opposite to the local intrinsic wave group velocity. In the dimensionless terms of the present formulation this is equivalent to

$$\eta_\infty = -\frac{1}{\Lambda} \tag{12}$$

12

or,

$$\eta = -\frac{1}{4\Lambda}. \tag{13}$$

These conditions are conservative and they are independent of the precise value of the wave ampli-
tude, and the wave amplitude defined by these conditions is infinite. In a continuous refraction pro-
cess, waves break well before these boundaries are reached, and more energy and momentum are lost
to wave breaking than is indicated by the above conditions. It is more realistic to establish the wave
breaking boundary in some manner based on a local wave steepness condition (see, for example,
Ramberg and Griffin (1987) and Ochi and Tsai (1983)). These represent criteria which depend both
on the initial spectral distribution and the integrated growth of the particular spectral component.

The wave-breaking boundary is utilized to establish limits of integration for the mean square
surface elevation energy $<\zeta^2>$ or, equivalently, limits for the contributions to the surface elevation,
ζ. Utilizing Eq. (13) as the definition of the wave breaking boundary θ_b the result is

$$\sin \theta_b = -\frac{1}{4\Lambda\omega^*}. \tag{14}$$

This establishes the lower integration limit for θ. For waves with components in the direction of the
current, $\theta > 0$, interaction with the current can produce reflected waves. Waves which are about to
reflect are characterized in the physical plane at $\theta = \pi/2$.

To obtain some insight into the spectral distribution throughout the interaction zone the contribu-
tions from various ranges of wavelengths to the surface energy must be quantified. This necessitates
establishing modified limits of integration for the energy integral previously developed. The locus of
constant wavelength within the interaction zone in either the initial or physical plane is given by

$$\sin \theta_\infty = \frac{g}{\Lambda V_m \, \omega_\infty} \left[\frac{\omega_\infty - \sqrt{kg}}{\omega_\infty} \right] \equiv \sin \theta_k. \tag{15}$$

This equation provides the value of θ_∞ which produces for a total frequency ω_∞ a wave number of k
at a position y where the local current is given by $V_m \Lambda(y)$, and it therefore defines the required
locus in the initial plane. Equation (15) is used to establish the required limits of integration for the
surface energy as discussed above. Of course, the limitations imposed by Eq. (15) have to be incor-
porated with respect to those limitations already associated with wave breaking and wave reflection.
In the above equations Φ_∞ represents the spectral density of the ambient random wave field. The
simplest case corresponds to a spectrum similar to that of white-noise

$$\Phi_\infty \, (\omega_\infty, \, \theta_\infty) = \text{constant},$$

when the constant may be taken as unity without any loss of generality. This was the original
approach taken by James et al (1977). More importantly, other random sea state spectra may be used
for Φ_∞ such as those of Pierson-Moskowitz, JONSWAP etc., and the recently-proposed model of
Phillips (1985). For example, the frequency-direction spectral density of Pierson-Moskowitz is given
as

$$\Phi_\infty \, (\omega_\infty, \, \theta_\infty) = \frac{C}{\omega_\infty^6} \exp \left[\frac{-.74g^4}{U_w^4 \, \omega_\infty^4} \right] \cos^p \left[\nu \, (\theta_\infty - \psi_w) \right], \tag{16}$$

13

where U_w represents the wind velocity, ψ_w represents the wind direction, ν and p are parameters typically equal to 1 and 2, respectively, and C is a constant. The ω_∞^{-6} behavior of Eq. (16) is consistent with the spectral density as defined by Eq. (3). The various models in common use are described by Wang (1985) and Phillips (1985).

KELVIN SHIP WAVES

In many surface hydrodynamics applications it is of interest to predict the wave-making resistance of a particular ship hull and the resulting free surface ship wave pattern. Such predictions can be used for the analysis and study of the hull design and its wake characteristics. To meet this need, the far-field ship wake computer program FFSW has been developed. A detailed description of this program and discussion of the theory implemented to develop the computational model can be found in Keramidas and Bauman (1987).

The computational model employed in the computer program is based on Slender Ship theory (Noblesse, 1983) with a number of improvements over existing computer programs which employ the same theory. These improvements allow for a more accurate description of hull geometry and panel generation. The computer program is divided in three major parts: a) Input, geometry (panel) generation and source strength generation; b) Wave spectra, wave resistance and wake calculations; and c) Output for printer or disc file. The FFSW program is completely interactive and menu driven, so that it requires only minimum user interface.

The implementation of the Slender Ship theory into a useable computational tool consists of several steps. Each of these steps provides the necessary input to the computational model for obtaining numerical results for the wave resistance and the Kelvin wave field. The first and probably the most important step is the generation of the surface panels and the specification of the source strength densities; the accuracy of the calculations depends a great deal on the accurate representation of the ship hull surface by the panels as well as as the accurate specification of the unit normal vector on each of the panels. A set of algorithms has been written to perform both the panelization of the hull surface and the calculation of the unit normal. The algorithm for the latter produces results for both the surface area of each panel and the unit normal. This is a much improved algorithm over existing ones, since it takes into account the curvature of the panel. The input information required to perform the panelization process is obtained from a data file which contains the offset lines of the particular ship hull under consideration.

Two sets of calculations are possible; the first set of calculations that one can perform is of the wave spectra, for a given ship hull configuration and for a specified number of ship speeds. Wave making resistance is then calculated from the wave spectra results and can be saved as an output file: the second set of calculations includes the free surface elevations of the far field wake as well as both x- and y-slopes.

SHIP WAVE MODIFICATIONS

The theoretical model employed here is essentially that of Peregrine (1971) as modified by Griffin (1988). It is assumed that the relatively short, divergent waves generated at the stern of the ship (source) move away from the center line of the wake as they are refracted by the mean flow, and that they pass through only a small region of the wake. The source is assumed to represent the stern region as the chief source of wave generation in the pattern. It is understood, however, that in many cases waves generated at the ship's bow also may contribute to the overall wave system.

The wake is assumed to be narrow relative to the lateral dimension of the far-field wave pattern and to be uniform or at most slowly-varying with downstream distance from the moving source. This assumption places stringent limitations on the allowable extent of the surface current profile. In a practical sense this limits the origin of the flow to the wake caused by the passage of the ship (typically the wake is approximately two to five ship beams in width). Naturally-occurring surface current fields generally are greater in extent. These are reasonable assumptions under most circumstances. The moving source is assumed to generate waves of all frequencies, but only the ship waves which are steady and move with the source speed are considered in the model. It is the well-known divergent cusp waves which are most visible near the boundaries of the Kelvin ship wave pattern, and it is the general pattern and modifications of these waves which are predicted here.

A coordinate system is chosen with x along the center of the wake or the ship track, y normal to the ship track, and z vertically downward. The undisturbed free surface is located in the plane $z = 0$. The wavemaking source is assumed to have a steady velocity U in the x direction. The wake is represented in its most general form by a velocity distribution $u(y,z)$ with the properties $0 < u(y,z) < U$ for $-d < y < +d$ and $u = 0$ for y outside of this region. Assume that the source-generated waves have traversed the wake region and are propagating away freely in still water, i.e., there is no appreciable ambient surface wave field. Then if the wave pattern is steady and moving with the velocity U, individual wave components satisfy the relation

$$c = U \cos \theta, \tag{17}$$

where c is their phase velocity and θ is the angle that their direction makes with the x direction.

The wave energy is propagated inside the wake at a velocity which is equal to the sum of the group velocity normal to the wave crests and the local velocity $u(y)$ of the water. Based upon the previous work of Peregrine (1971) and of Longuet-Higgins and Stewart (1961), the properties of the refracted waves inside the wake are

$$c_1(y) = \frac{c^2}{c - u(y) \cos \theta} \tag{18a}$$

and

$$\cos \theta_1(y) = \frac{c^2 \cos\theta}{(c - u(y) \cos \theta)^2}. \tag{18b}$$

Here the subscript 1 denotes values of the wave properties inside the wake and the absence of the subscript denotes the freely moving waves outside of the wake.

If the substitution

$$W(y) = 1 - u(y)/U \tag{19}$$

is made and Eq. (17) is introduced, then

$$c_1(y) = c/W(y), \quad \cos \theta_1(y) = \cos \theta/W^2(y).$$

The group velocity in deep water is equal to half the phase velocity, so that within the wake a wave packet has the velocity

$$\left[u(y) + \frac{U \cos^2 \theta}{2 \, W^3(y)} \, , \, \frac{U \cos \theta \, [W^4(y) - \cos^2 \theta]^{1/2}}{2 \, W^3(y)} \right].$$

If the source is at the origin at the time $t = 0$, then the waves generated when the source was at $(-Ut, 0)$ have a locus in the x, y plane given by

$$x = -Ut + \frac{1}{2} \, Ut \, \cos^2 \theta + \int_o^d \frac{[(1 - W^3(\zeta))\cos^2 \theta + 2 \, (1 - W(\zeta))W^3(\zeta)]d\zeta}{\cos \theta \, [W^4(\zeta) - \cos^2 \theta]^{1/2}} \qquad (20a)$$

$$y = d + \frac{1}{2} \, Ut \, \sin \theta \cos \theta - \int_o^d \frac{W^3(\zeta) \, \sin \theta \, d\zeta}{[W^4(\zeta) - \cos^2 \theta]^{1/2}} \qquad (20b)$$

for that part of the pattern with $y > d$. The envelope of the wave pattern given by the equations

$$x = \int_o^d \frac{[1 - W^4(\zeta)] \, \cos^3 \theta \, [3 \cos^2 \theta - 2 - 2 \, W^4(\zeta)] \, d\zeta}{(2 - 3 \cos^2 \theta)[W^4(\zeta) - \cos^2 \theta]^{3/2}} \qquad (21a)$$

$$y = d + \int_o^d \frac{W^4(\zeta) \, \sin^3 \theta \, [3 \cos^2 \theta - 2W^4] \, d\zeta}{(2 - 3 \cos^2 \theta) \, [W^4(\zeta) - \cos^2 \theta]^{3/2}}, \qquad (21b)$$

which are derived by eliminating the time t from Eqs. (20) and taking the derivative $\partial/\partial\theta$ of the resulting intermediate equation (Peregrine, 1971). This envelope is valid for an arbitrary surface-plane ($z = 0$) velocity profile $u(y)$ over the total wake width $2d$. The refracted steady wave pattern corresponding to such a profile can be computed numerically using Eqs. (20) to give the pattern of the wave crests. The corresponding Kelvin wave amplitudes for a single moving source can be determined by combining the approach taken by Munk et al. (1987) with the present one.

Lines of constant phase in the wave pattern are given by the equation

$$X = \mathbf{k} \cdot \mathbf{r} - \sigma t = k(x \cos \theta + y \sin \theta) - \sigma t.$$

In the present case for steady, deep water waves

$$c = U \cos \theta = \frac{\sigma}{k} = \frac{g}{\sigma},$$

so that the phase function is transformed to

$$X = \frac{g}{c^2} \, (x \cos \theta + y \sin \theta - ct),$$

or

$$X = \frac{g}{U^2 \cos^2 \theta} \, (x \cos \theta + y \sin \theta - U \cos \theta \, t). \qquad (22)$$

16

This equation represents a relation between t, θ and X when x and y are substituted from Eqs. (20a) and (20b).

There are a number of features of the overall modified ship wave pattern which can be obtained from the foregoing equations. At the time of Peregrine's original work there were virtually no experimental results with which to compare the predictions. This situation has changed somewhat as more wake observations have become available from airborne and spaceborne SAR and other forms of imagery. Thus even such a relatively simple approach can provide useful initial information and possible directions for more detailed further studies. A first approximation can be obtained by assuming that the surface current profile is given by $u(y) = V$, a constant, for $|y| < d$. Then no numerical integration is required and the equations for the envelope of the modified wave pattern simply reduce to

$$x = \frac{d(1 - W^4) \cos^3 \theta \, (3 \cos^2 \theta - 2 - 2W^4)}{(2 - 3 \cos^2 \theta) \, (W^4 - \cos^2 \theta)^{3/2}} \tag{23a}$$

and

$$y = d + \frac{d \, W^4 \sin^3 \theta \, (3 \cos^2 \theta - 2W^4)}{(2 - 3 \cos^2 \theta) \, (W^4 - \cos^2 \theta)^{3/2}}. \tag{23b}$$

It is instructive to look briefly at two special cases of these equations. Then some further calculations can be made for some cases of more general interest. The far field behavior of the waves is readily obtained from the above equations. The denominator on the right hand side of each equation must approach zero in order for x and y to increase without bound as the far field is approached. There are two ways in which this situation can occur.

Case One: $W^4 > 2/3$.

The denominators of Eqs. (7a, b) then are zero if

$$(2 - 3 \cos^2 \theta) = 0. \tag{24}$$

This reduces to the usual Kelvin ship wake pattern ($\theta = 35.3$ degrees and $\alpha = 19.5$ degrees) and represents what Peregrine has described as a 'weak' wake. The condition $W^4 > 2/3$ implies that $u < 0.1U$.

The envelope of the wave pattern is bounded by the asymptotes given by the line(s)

$$y = - \frac{\sin \theta \cos \theta}{1 + \sin^2 \theta} x \tag{25}$$

or, in terms of the half-angle α of the wake,

$$\tan \alpha = - \frac{\sin \theta \cos \theta}{1 + \sin^2 \theta} = - \frac{1/2 \tan \theta}{1/2 + \tan^2 \theta}. \tag{26}$$

Here the angle α is given by

$$\alpha = \arc \tan \left(\frac{y}{x} \right).$$

Equation (25) has been shown by Crapper (1984), Newman (1977) and by Lighthill (1979), among others, to represent the usual Kelvin wave pattern for a ship moving in still water.

Case Two: $W^4 < 2/3$.

For this case the denominator is zero if

$$\cos^2 \theta = W^4. \tag{27}$$

This condition results in a larger value of θ than for the unmodified Kelvin wave pattern. The angle θ of the modified divergent wave system varies over only a relatively small range as compared to the previous case since, at $y = d$, the limiting value is given by

$$\cos^2 \theta_{max} = 2/3 W^4. \tag{28}$$

This gives the maximum value of the angle θ for a wake condition represented by the current field of strength W. The behavior of the waves at infinity also can be determined in a similar manner from the full Eqs. (20a,b) as shown by Peregrine (1971).

Not only the angular extent and phase, but also the characteristic lengths of the divergent wave pattern are altered by the presence of the current. The modified lengths of the steady waves in the pattern are given by

$$\lambda = \frac{2\pi U^2}{g} \cos^2 \theta. \tag{29}$$

In terms of the reference Kelvin wave length λ_0 for a given set of conditions, the divergent, small wavelength portion of the ship waves at the outer edge of the v wake is given by

$$\frac{\lambda}{\lambda_0} = \frac{W^4}{\cos^2 \theta_0}, \tag{30}$$

where $\cos^2 \theta_0 = 2/3$. Equation (13) can be recast in the form

$$\lambda / L = 2\pi \left[U^2 / gL \right] \cos^2 \theta = 2\pi F^2 \cos^2 \theta. \tag{31}$$

for a ship of length L and Froude number $F = U / \sqrt{gL}$. In terms of the wake half-width d,

$$\lambda / d \cdot d / L = 2\pi F^2 \cos^2 \theta.$$

The limiting value of $\lambda / d = 1$, since within the limitations of the present simplified theory the wavelength λ should be less than the wake half-width d. Then the above equation reduces to

$$d / L = 2\pi F^2 \cos^2 \theta.$$

The half-width d is approximately equal to the ship's beam B (since, empirically, $2d = 2$ to $3B$), which gives the result

$$B / L = 2\pi F^2 \cos^2 \theta.$$

For a typical ship $B / L = 0.10$ to 0.15, so that we may choose as a representative value $B / L = 0.13$. When the half-angle of the modified Kelvin wake is $\alpha = 14$ degrees, the wake velocity parameter $W^4 = 0.25$ and the wave direction angle is $\theta_{max} = 66$ degrees. Introducing these numbers into Eq. (31) gives

$$F^2 = 0.122; \quad F = 0.35$$

as the limiting value of the Froude number for these conditions. Thus this relatively simple theory can represent a first approximation for a realistic surface ship condition as represented by the Froude number. The Froude number of the high-speed destroyer (model and full scales) is $F = 0.28$ for the conditions considered here.

LIMITING WAVE STEEPNESS

If the limiting wave steepness s_L is specified in some manner, then, for given ambient conditions a_∞, k_∞, ω_∞ where $u = 0$, the solution of the governing model equations gives the local surface shear current which accompanies the onset of wave breaking. A reasonable estimate of the expected local steepness $s = ak$ at the onset of breaking is $s_L = 0.34$ (Ramberg and Griffin, 1987). The classical Stokes criterion for the breaking of steep, symmetric waves in deep water has been computed by numerous investigators and is $s_L \cong 0.446$. This is another conservative criterion for predicting the onset of breaking since it represents fewer breaking waves in a given record. An even more conservative approach is that of James et al. (1977). The breaking condition there is taken to be the vanishing of the local absolute group velocity C_g. Then the opposing current at the breaking condition is given by

$$u(y)\sin\theta = -c_g. \tag{32}$$

where c_g is the local intrinsic group velocity ($c_g = \sigma / k$).

The principal problem which arises in trying to implement any criterion is the specification of the incident or ambient and breaking wave steepnesses. For monochromatic incident waves as in a laboratory channel the problem is a relatively minor one. Both the initial steepness and the limiting steepness at the onset of breaking are relatively easy to measure and to characterize (Melville, 1982; Su et al., 1982; Ramberg and Griffin, 1987).

The onset of breaking or the limiting steepness for deep water waves can be predicted by combining measured laboratory-scale breaking wave limits with some acceptable form of the ambient or incident spectrum. From a practical standpoint this approach provides a reasonable estimate based upon direct measurements of individual breaking events. Such an approach is based upon the original work of Longuet-Higgins (1969), Nath and Ramsey (1976) and of Kjeldsen and Myrhaug (1978). Ochi and Tsai (1983) have measured individual breaking events for steep nonlinear waves and have introduced more realistic wave spectra into the formulation. This approach to specifying the limiting or onset condition also is discussed by Ramberg and Griffin (1987), Huang et al. (1986), and Srokosz (1986).

Increased steepness and/or breaking of the waves are strong contributors to the enhanced wake signature. The recent experiments of Banner and Fooks (1985) have shown that breaking surface waves can significantly influence the radar cross-section (RCS) of the ocean surface.

A brief summary of the approach and a conceptualization of how it may be introduced into the present formulation is given here. The ratio of the incident, or ambient, and breaking wave steepnesses is given by

$$\frac{s_\infty}{s_L} = \frac{a_\infty k_\infty}{a_L k_L}.$$

19

This ratio can be expressed in the equivalent form

$$\frac{s_\infty}{s_L} = \frac{(H_\infty/\lambda_\infty)}{(H_L/\lambda_L)} \tag{33}$$

since the crest-to-trough wave height $H = 2a$. For the ambient waves in deep water the dispersion relationship gives $\omega_\infty^2 = g k_\infty$. At the onset of wave breaking the Stokes limiting wavelength is

$$\lambda_L = (1.2g/2\pi)T_L^2, \tag{34}$$

so that the ratio of wave steepnesses can be further reduced to the form

$$\frac{s_\infty}{s_L} = \frac{(H_\infty/T_\infty^2)}{(H_L/1.2T_L^2)}. \tag{35}$$

Here T_∞ and T_L respectively are the wave periods of the ambient and local limiting waves.

The steepness criterion for the onset of wave breaking in deep water as stated by Ramberg and Griffin (1987) is

$$H \geq \alpha g \, T^2, \tag{36}$$

where α is an empiracally determined threshold parameter. The most comprehensive measurements available at the present time indicate that $\alpha = 0.021$. Then the ratio of wave steepnesses reduces to

$$s_\infty/s_L = 1.2 H_\infty/\alpha g T_\infty^2 \tag{37}$$

and is expressed in terms only of the threshold parameter α and a characteristic height H_∞ and period T_∞ of the ambient or incident waves.

Srokosz (1986) has introduced a related criterion for the onset of wave breaking, or for the limiting wave height or steepness. It is assumed that the wave will break if the downward acceleration of the crest exceeds βg, where β is another positive threshold parameter. Longuet-Higgins (1963, 1969) has demonstrated on theoretical grounds that the acceleration at the crest of the highest wave is 0.5g, so that a reasonable choice based directly upon theory is $\beta = 0.5$. It is straightforward to show that there is a correspondence between Eq. (36) and the maximum acceleration at the crest. Given that

$$H \geq \alpha g T^2,$$

and assuming again as a first approximation that $H = 2a$, then Eq. (36) takes the form

$$2a \geq \alpha g \left[\frac{2\pi}{\omega} \right]^2$$

or equivalently that

$$a\omega^2 \geq 2\pi^2 \alpha g. \tag{38}$$

The left-hand side of this equation is the acceleration of the wave crest to a good approximation, so that

$$\beta = 2\pi^2 \alpha. \tag{39}$$

20

Taking the experimentally-determined value of $\alpha = 0.021$, the parameter $\beta = 0.41$. Thus the limiting acceleration of the wave crest at the onset of breaking is 0.41g based upon experiment, whereas the limiting acceleration is 0.5g based upon theory (Longuet-Higgins, 1963, 1969).

There are a number of ways to specify H_∞ and T_∞. Ochi and Tsai (1983) set H_∞ proportional to the rms wave height and T_∞ equal to the average time between positive maxima for a narrow-band spectrum. Kjeldsen and Myrhaug (1978) simply set H_∞ and T_∞ equal to the rms wave height and period of the wave field. Unlike the simple criterion of Eqs. (12) and (13), the effects of wave breaking are not confined to a local region in wave number or frequency-direction space. At present we are investigating means to introduce this type of non-local criterion into the wave-current interaction model, and a brief discussion is given later in the report.

DISCUSSION OF RESULTS

Kelvin Ship Waves

The results to be presented in this section include a brief discussion of the far field Kelvin waves generated by a ship in forward motion. The formulation used for calculating the Kelvin wave field is based on Slender Ship theory (Noblesse, 1983) and numerical results were obtained using the computer program FFSW (Keramidas and Bauman, 1987). The numerical results from FFSW provide predictions for three quantities relevant to the far field Kelvin wave field; these are the wave elevations, and the x- and y-slopes of the wave elevations.

The availability of recent model-scale experimental data for the high speed destroyer hull with a sonar dome (Model 5415) makes it opportune to use this generic hull in the present study to predict its Kelvin wave field and its wave modifications. The first set of results that is presented in this report was obtained from the free surface calculation using FFSW. In Fig. 6 the results obtained for the far field Kelvin waves are shown. The calculations extend downstream from the stern of the ship to about five ship lengths and two ship lengths on each side in the cross stream direction. The results were obtained for a full-scale speed of 20 knots (10 m/s), which corresponds to the model experiment (see Table 1). Figure 6a shows the actual wave elevations in a perspective view, and Fig. 6b shows the contours of constant wave amplitude. The second set of results is given in terms of wave slopes. As was mentioned above, the program output generates the x and y slopes of the wave elevations, which are proportional to the respective directional wave numbers. In Fig. 7 the total slopes are presented, or the magnitudes of the product of the wave number and the amplitude. These results are more relevant to radar imagery than are the actual wave elevations. By comparing Figs. 6b and 7 one can see that they have different characteristics and that certain features of the Kelvin wave field are present only in Fig. 7.

From recent Kelvin wave observations the presence of the narrow v angle, smaller than the usual 19.5 degree value, has been observed as described earlier in the report. In Fig. 7 one can notice the presence of such an angle being formed by the contours of the wave slopes between $ak = 0.14$ and 0.34. This result is encouraging and may have some bearing on the overall v wake question, but further investigations are required. Another possible cause of the narrow-v angles observed in the radar imagery is discussed in the next section of the report. The final set of results for the Kelvin wave field of the high speed destroyer is presented in Fig. 8 in terms of two wave cuts; the first about one beam distant from the centerline of the wake and the second at two beams distant. These results illustrate the magnitude of the wave field generated by the passage of the ship, at the forward speed of 20 kt (10 m/s).
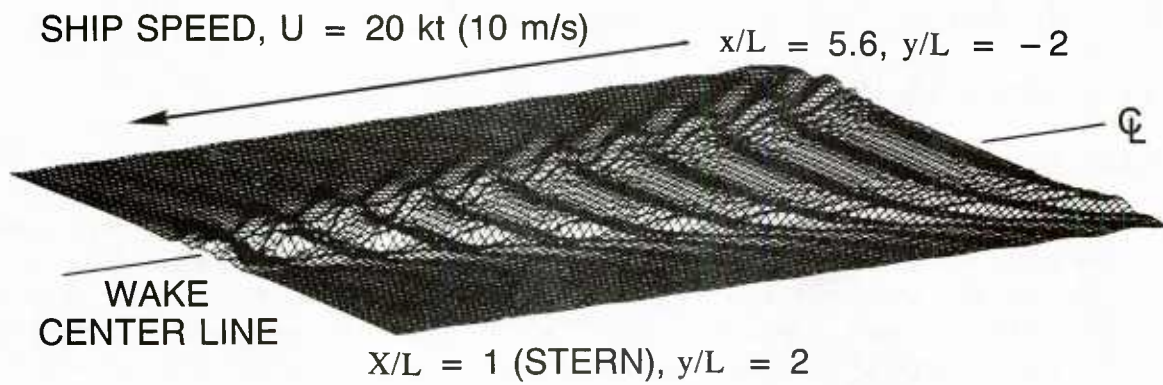
Fig. 6(a) — The Kelvin ship wave pattern in the wake of a twin-screw high speed destroyer in steady motion at a forward speed of 20 kt (10 m/s).

A three dimensional surface plot of the wave field.
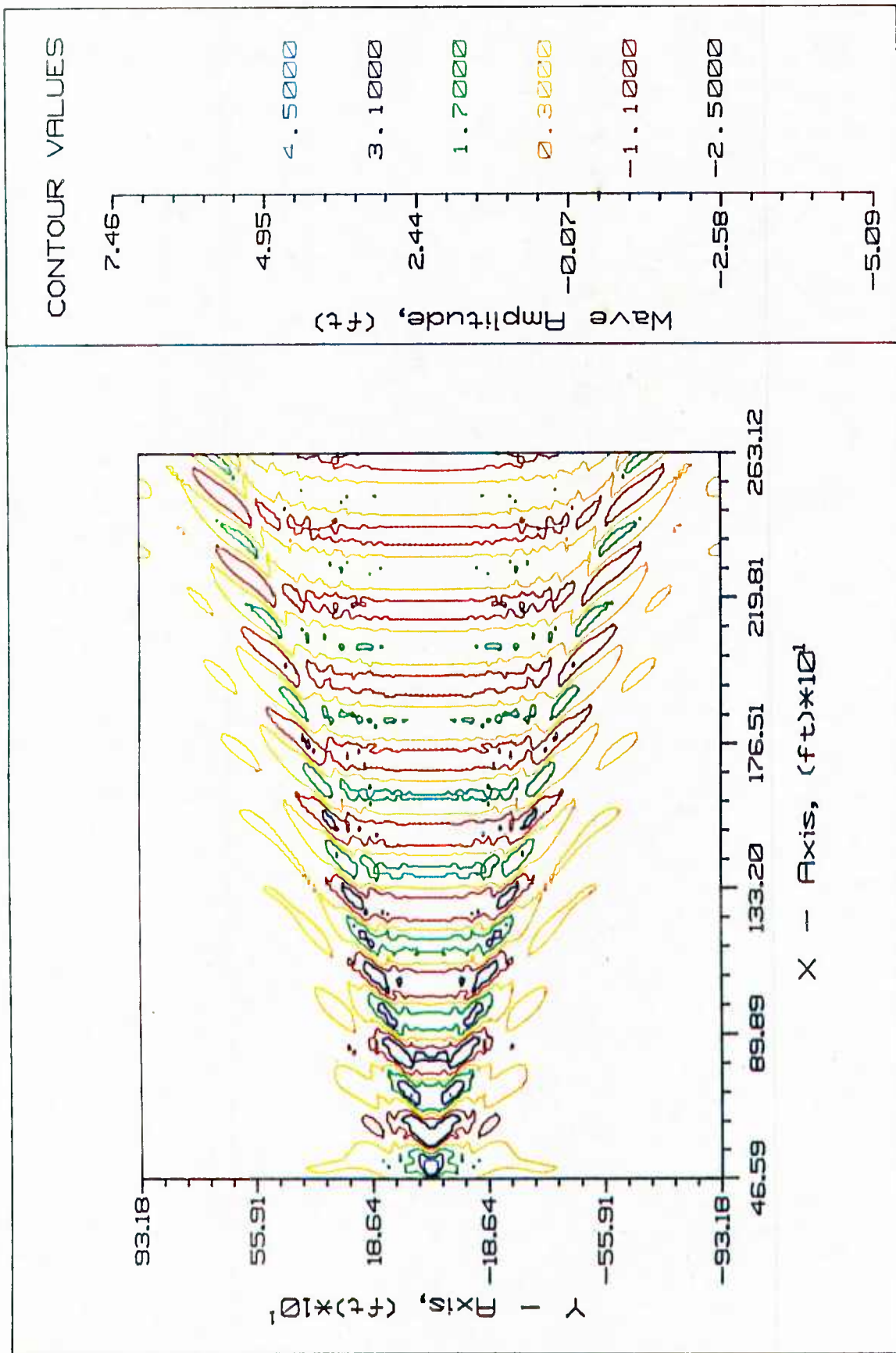
Fig. 6(b) — The Kelvin ship wave pattern in the wake of the a twin-screw high speed destroyer in steady motion at a forward speed of 20 kt (10 m/s). (1 ft = 0.305 m)

Contours of constant wave amplitude.

23
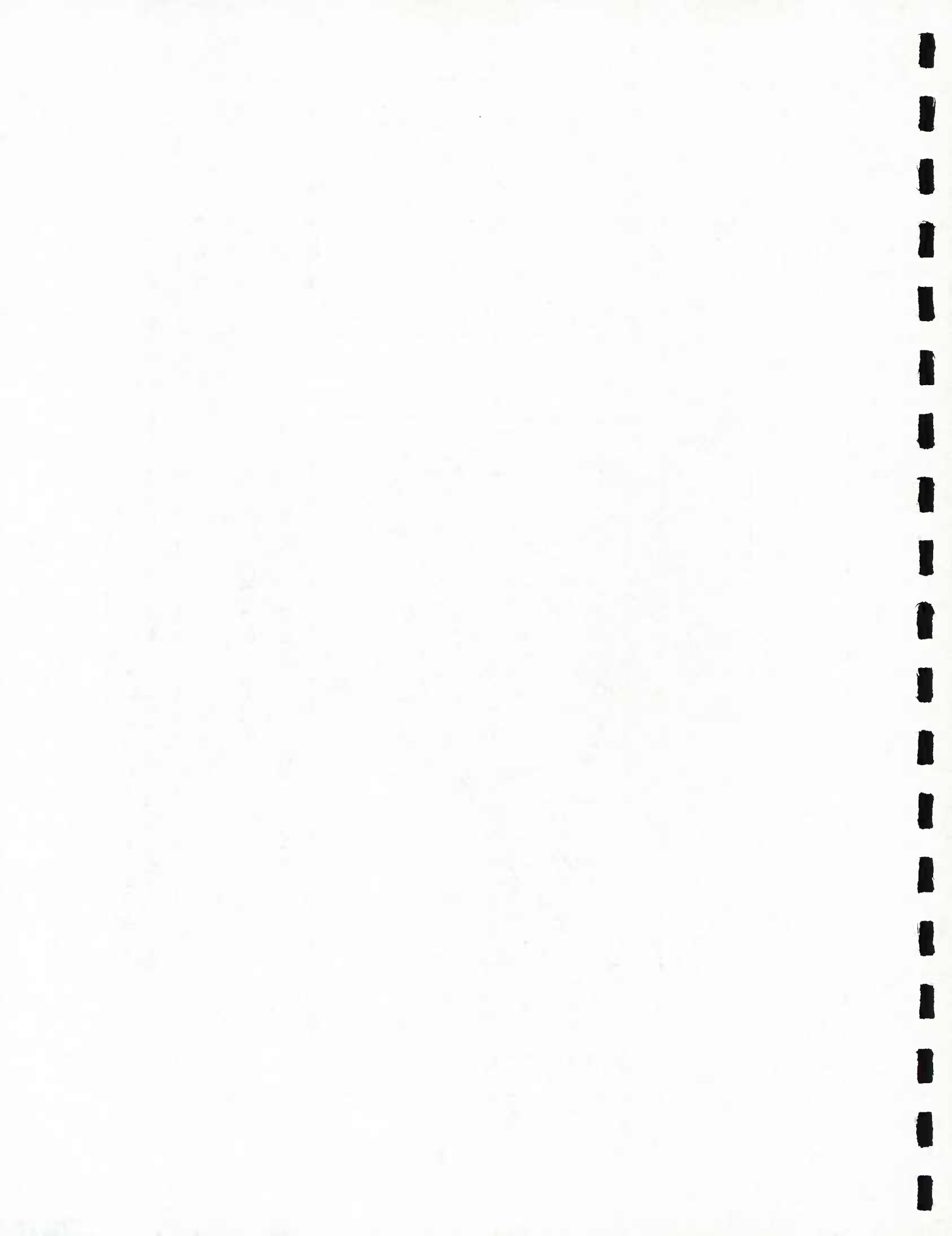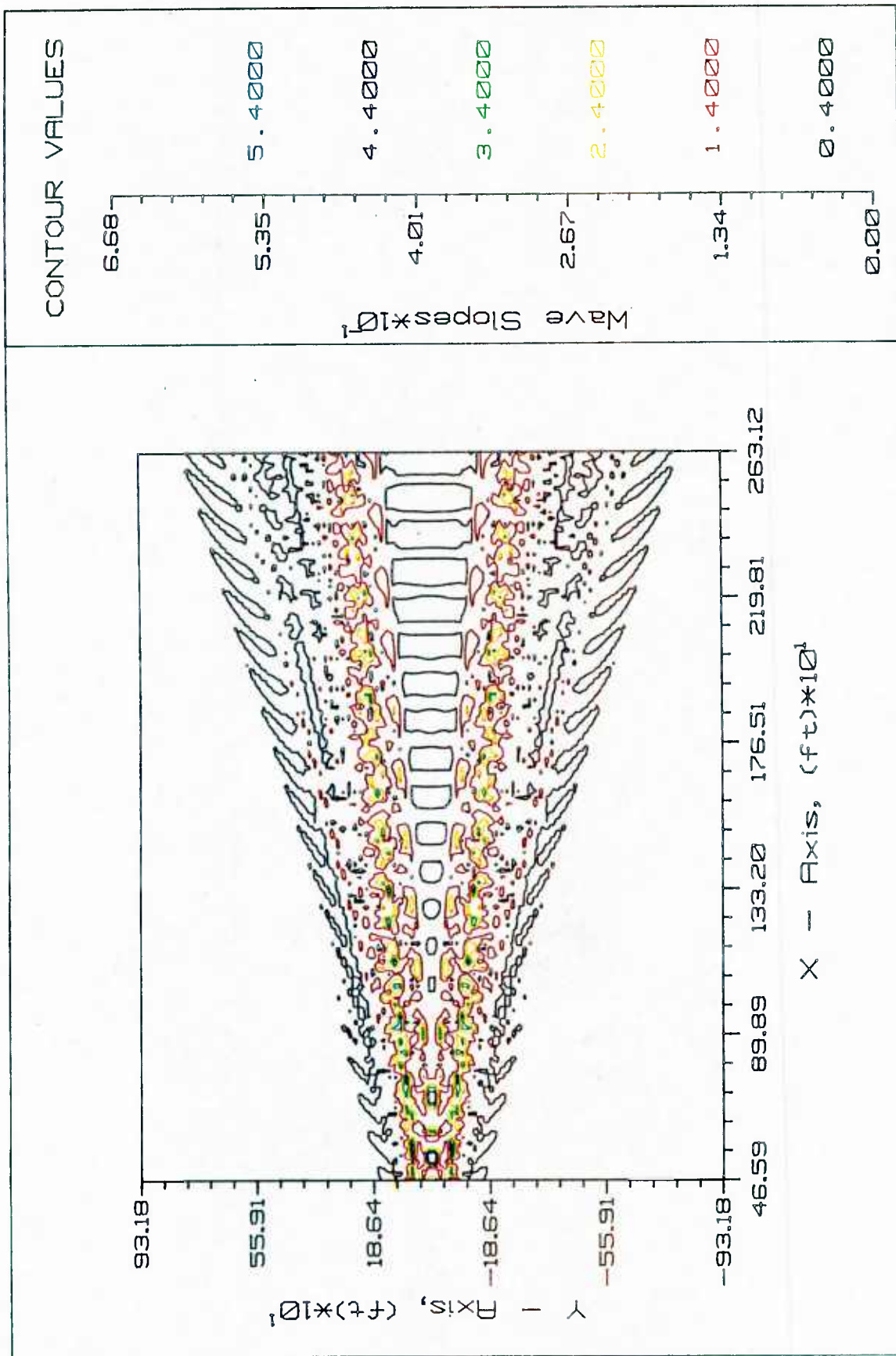
Fig. 7 — A contour plot of the wave slopes *ak* in the wake of a high speed destroyer at 20 kt (10 m/s). (1 ft = 0.305 m)
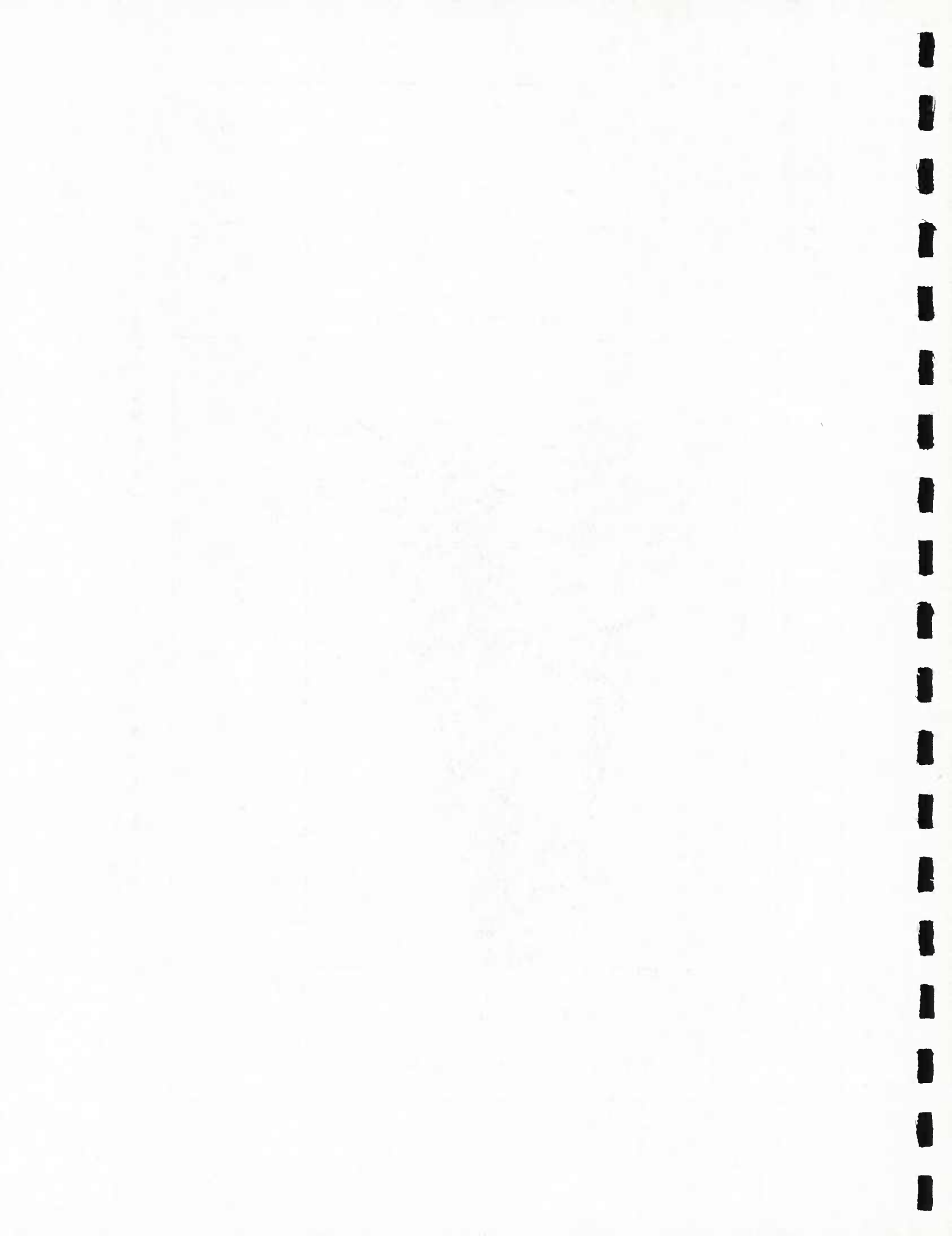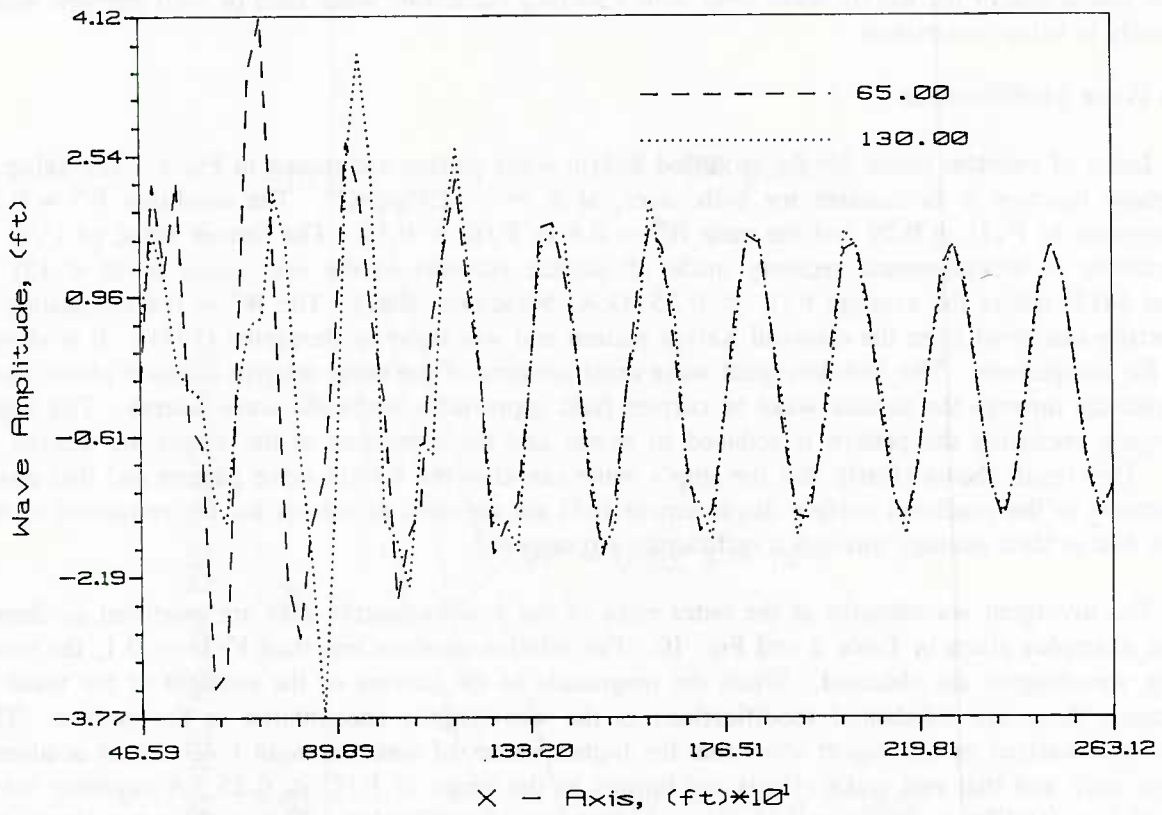
Fig. 8 — Longitudinal wave cuts in the Kelvin wake of a high speed destroyer at 20 kt (10 m/s). (1 ft = 0.305 m)

Table 2 — Ship Wave Modification by a Surface Wake Flow Field
(Divergent Waves)

Wake Half-angle, α (deg)	Relative Current, V/U	Ship Speed, V (k t)	Wavelength, λ (m)	
16	0.23 $(W^4 = 0.35)^+$	12	8.48	$(\lambda/\lambda_0 = 0.53)$
		8	3.76	
		4	0.95	
14	0.29 $(W^4 = 0.25)$	12	6.20	$(\lambda/\lambda_0 = 0.38)$
		8	2.75	
		4	0.69	
12	0.37 $(W^4 = 0.16)$	12	3.84	$(\lambda/\lambda_o = 0.24)$
		8	1.71	
		4	0.43	
6	0.55 $(W^4 = 0.043)$	12	1.02	$(\lambda/\lambda_o = 0.064)$
		8	0.46	
		4	0.11	
4	0.63 $(W^4 = 0.029)$	12	0.47	$(\lambda/\lambda_o = 0.029)$
		8	0.21	
		4	0.052	

$^+ W = 1 - V/U$
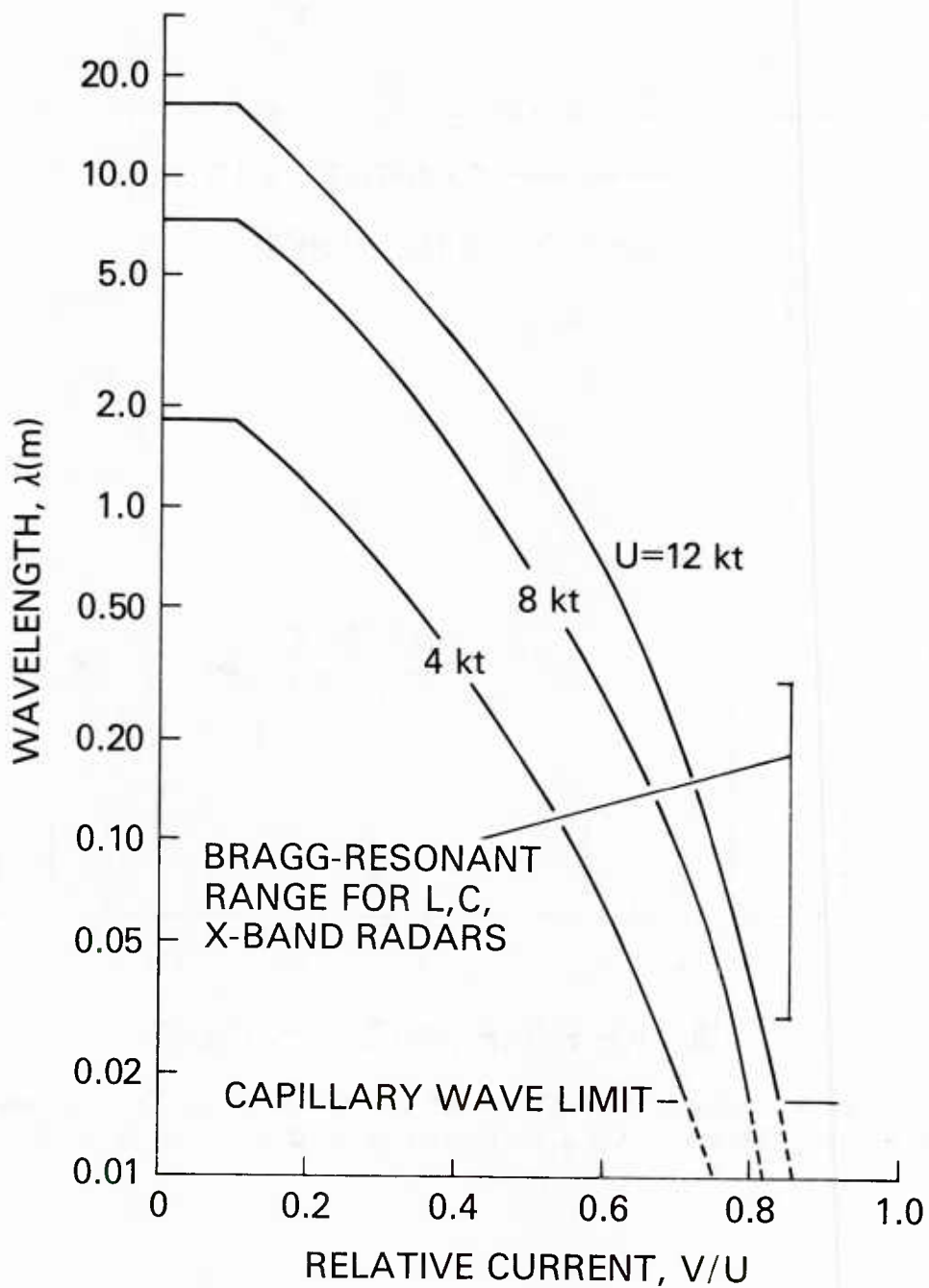
Fig. 10 — Typical wavelengths of the divergent waves in the modified surface ship wake as a function of the current/ship speed ratio V/U. For $V/U < 1/10$, the wavelengths are those of the unmodified Kelvin wake.

31
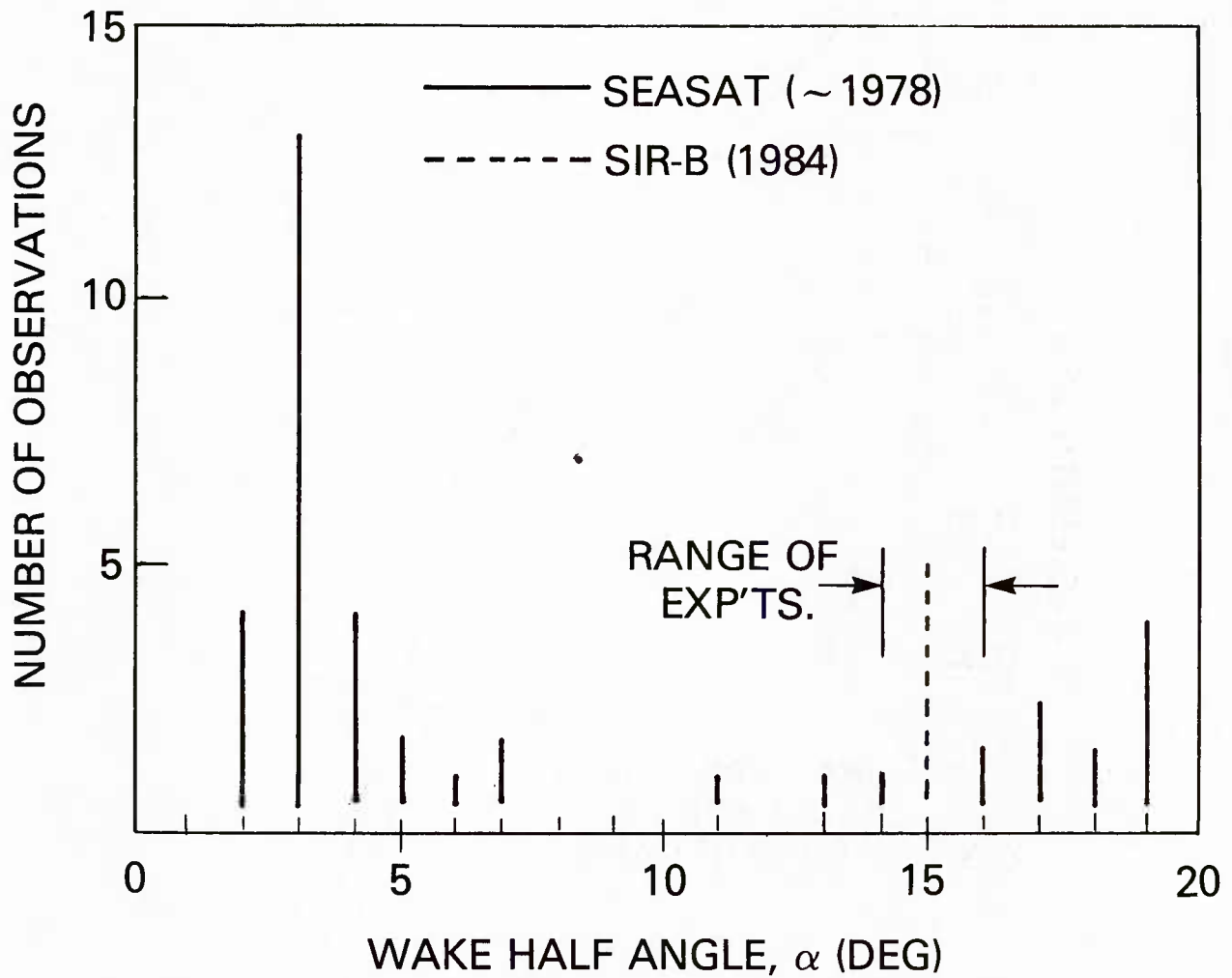
Fig. 11 — Observed distribution of SEASAT and SIR-B ship wake angles (SEASAT results adapted from Hammond et al., 1985). The SIR-B results were provided by Dr. A. M. Reed of DTRCEN (1986).

Ambient Wave Modifications

The results to be discussed in this section of the report include sample calculations of the modification of a random deep water wave field by the presence of a surface current pattern $U(y)$. The general features and dimensions of the surface region containing the current correspond to the surface wake of a full-scale destroyer. The width of the current field is 56 meters. This is nominally 2.5 ship beams, for B/L = 0.133 as in the case of the high speed destroyer of length L = 143 m (470 ft). The maximum value of the surface current is chosen to be V_M = 75 cm/sec (1.5 kt), which is representative of the full-scale ship wake as scaled up from the model tests and computations. This is 7.5 percent of the full-scale ship speed of 20 kt, a condition which corresponds to the surface mean flow (relative to still water) at one-half ship length astern. The results largely have been chosen to demonstrate the effectiveness of the wave-current interaction in eliminating the short wave components. For example, the wave number range of k = 0.2 to 1 cm^{-1} in deep water is comparable to the operating wave number ranges of L-, C- and X-band radars.

A Sea State Four/Five ambient wave field was chosen for the computations using a Pierson-Moskowitz spectrum with cosine-squared spreading as an example. The computational grid in all of the examples consisted of an array of 51 × 51 points. The nominal wind speed used in the simulation was U = 12 m/sec (24 kt). The patch of ocean surface measured 70 m × 70 m, with the surface wake or current field covering the central 56 m in the y or cross-wake direction. This corresponds nominally to the wake dimensions discussed in the previous paragraph, although the simulation is somewhat of an idealization because a simple parabolic variation of the surface mean velocity over the surface wake was employed. The horizontal x and y directions are scaled by the factor g/V_M^2.

Figure 12 shows the surface wave pattern for wave numbers between k = 0.2 and 1 cm^{-1} when the prevailing wave system is in the same direction as the surface flow pattern. This is the most effective relative orientation of the wave and current systems for reducing the short wavelengths (Cooper et al., 1987). The modified wave pattern includes all wave numbers greater than k = 0. The maximum peak-to-trough wave height H_{rms} = 1.1 cm is over the limited short wave number range investigated in this example. There is a clear reduction in the short wavelengths over the extent of the surface wake pattern as compared to the region outside of the wake.

When the wave number interval is expanded to k = 0.0005 to 3 cm^{-1}, the surface wave pattern is as shown in Fig. 13. The surface corresponding to all wave numbers greater than k = 0 now takes on the appearance of a random sea, with a maximum wave height H_{rms} = 121.2 cm. There are no visually identifiable regions of wave modification in the surface pattern, as in the short wavelength case, but the wave spectra in the current field are modified as shown below.

The strength of the surface wake diminishes sharply as the distance astern of the ship is increased. At a downstream distance of approximately twelve ship beams (1.5 ship lengths), the maximum surface mean velocity is about one percent of the ship speed, or 10 cm/sec (0.2 kt). The surface pattern in the short wave regime (k = 0.2 to 1 cm^{-1}) is shown in Fig. 14, again for all wavelengths in the modified pattern greater than k = 0. There is little evidence of a diminished short wave population in the wake region, so that a reduction in the radar backscatter from the surface is not likely to occur under these conditions.

Another example is shown in Fig. 15 for the case when the directions of the surface current field and the wave system are oriented at ninety degrees to each other. In this case there is no appearance of modification in the short waves in the range k = 0.2 to 1 cm^{-1}, although there is more energy in the system as denoted by the maximum waveheight in the field H_{rms} = 2.94 cm.
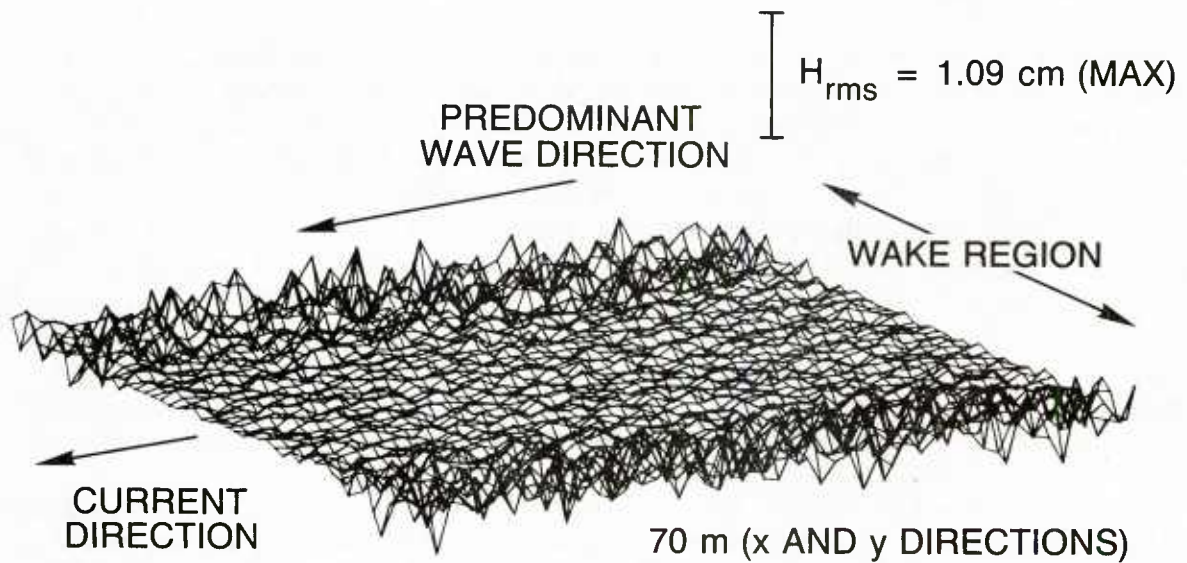
Fig. 12 — Spatial realization of the modified wave elevation in a surface wake or current field. The maximum surface velocity is $V_M = 75$ cm/sec. The horizontal field is 70 m in each direction, with the current field extending over the central 56 m. The ambient spectral density is Pierson-Moskowitz, with a wind speed of 12 m/sec (24 kt). All wave numbers greater than $k = 0$ in the modified field are shown, for incident wave numbers between $k = 0.2$ and 1 cm^{-1}. The waves and current are collinear and unidirectional.
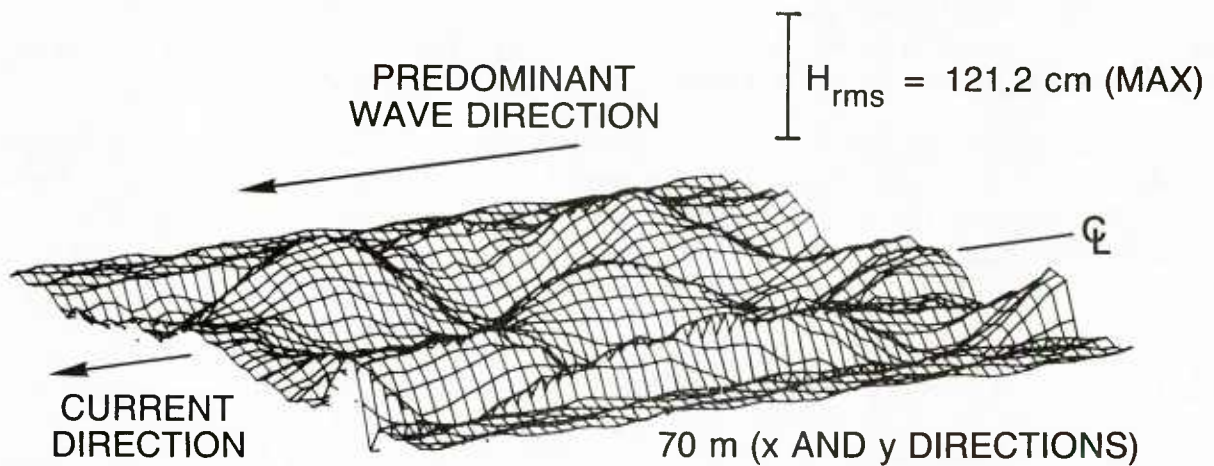
Fig. 13 — Spatial realization of the modified wave elevation in a surface wake or current field. Except for incident wave numbers between $k = 0.0005$ and 3 cm^{-1}, the conditions are the same as in Fig. 12.

$H_{rms} = 1.11$ cm (MAX)

PREDOMINANT
WAVE DIRECTION

CL

CURRENT
DIRECTION

70 m (x AND y DIRECTIONS)
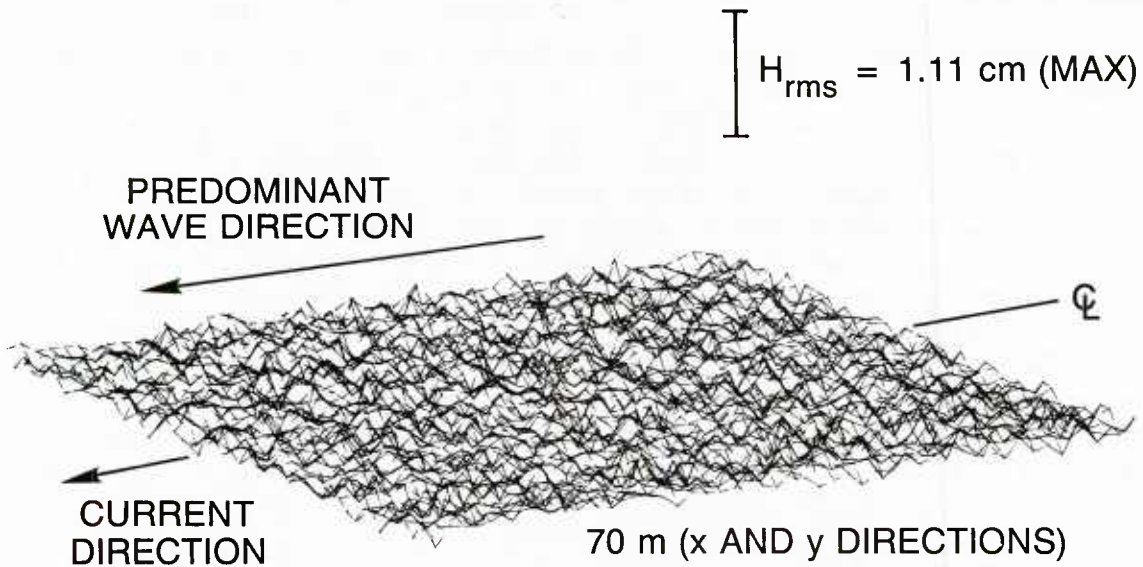
Fig. 14 — Spatial realization of the modified wave elevations in a surface wake or current field. Except for a maximum surface velocity of $V_M = 10$ cm/sec, the conditions are the same as in Fig. 12.

PREDOMINANT
WAVE DIRECTION

$H_{rms} = 2.94$ cm (MAX)

CL

CURRENT
DIRECTION

70 m (x AND y DIRECTIONS)
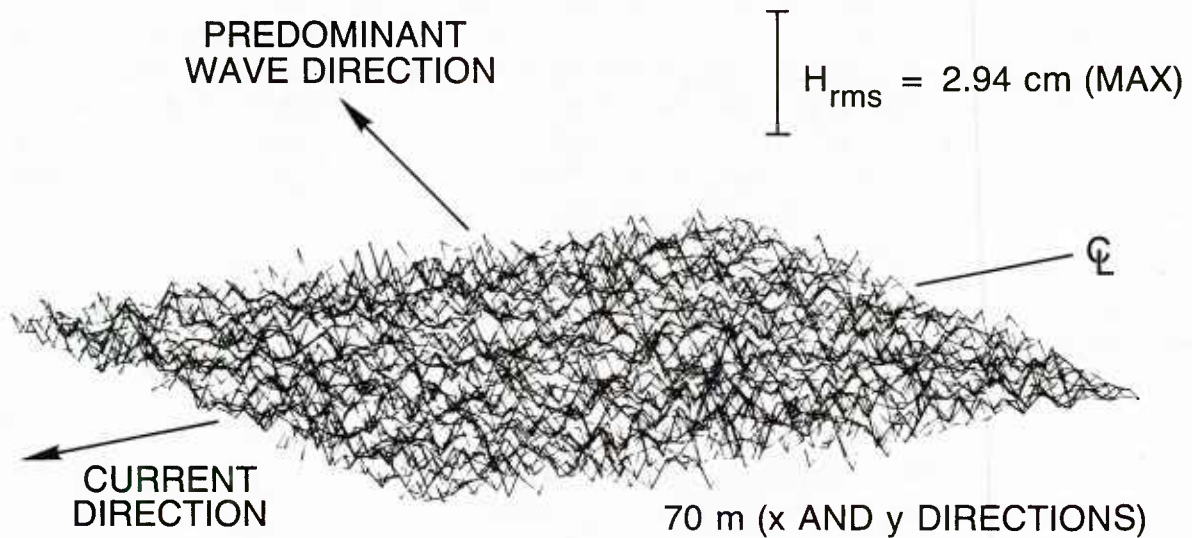
Fig. 15 — Spatial realization of the modified wave elevations in a surface wake or current field. The principal direction of the wave field is normal to the current; other conditions are the same as in Fig. 12.

This may be compared to the result in Fig. 12 when the waves and current were collinear and unidirectional.

Some sample calculations now are given for the frequency-direction spectral density in the modified surface wave pattern. Note that the form of the spectral density follows that of Eqs. (3) and (16), i.e. the frequency varies as ω^{-6}. The direction varies from $-\pi/2$ to $+\pi/2$, and the radian frequency ω is scaled by V_M/g. The frequency and direction are discretized into 25 and 24 points, respectively. Figure 16 qualitatively shows the variation in the spectral density across the wake when the wave system and the surface wake are collinear and unidirectional. The range of wave numbers in the initial plane is k = 0.0005 to 3 cm^{-1}, and the modified spectra correspond to all wave numbers greater than k = 0. The peak value in the spectral density is smallest at the wake center line y = 0 (the location of the maximum current) and increases as the cross-wake displacement is increased. The surface plot in Fig. 13 gives little evidence of the wave-current interaction, but the spectral densities indicate the modification of the wave field as the wake region is traversed in this, the strongest wake-wave interaction. The distribution of the wave energy is confined to angles between 0 and $+\pi$ with the predominant direction of the incident waves along the direction $\theta = +\pi/2$.

When the directions of the wave and current fields are normal to one another, there is little interaction between the two. This is demonstrated by the two spectra in Fig. 17, one from the center line of the wake and one displaced in the cross-wake direction. There is only a slight difference in the maxima in the spectra, but the angular distribution of the modified wave pattern is greater than in the previous example. The wave pattern is primarily in the direction $\theta = 0$ when the waves are normal to the wake flow.

Steep and Breaking Waves

The relatively simple wave breaking criterion represented by Eqs. (12), (13) and (32) yields a conservative estimate of the number of waves in a given record which are at the onset of breaking, since physically this onset condition occurs before the intrinsic group velocity c becomes equal and opposite to the current component in the wave direction $u(y) \sin \theta$ However, a dilemma arises in attempting to introduce a steepness criterion such as Eq. (36) into a local region of wave number or frequency-direction space. This is because the wave height H, and/or the wave period T are averaged globally in some manner as discussed earlier in the report.

One possible approach is to define the wave steepness in a local spectral representation (R. A. Skop, 1987). This can be accomplished in the following way. If the directional wave number spectral energy density is given by $S(k, \theta)$, then the local wave steepness is given to a good approximation by

$$k^p \ S(k, \theta) \sim a^2 k^2. \tag{40}$$

where p is an as-yet undetermined integer. When the onset condition for wave breaking, $H = \alpha g T^2$ or $ak = 0.34$, is introduced, the latter expression reduces to

$$k^p \ S(k, \theta) \sim 0.116,$$

which can be applied locally in wave number-direction space. A related formulation can be introduced in frequency-direction space. The wave number k is appropriately interpreted as the resultant value in the local wave direction. Steps are being taken at the present time to introduce such a less conservative onset criterion for wave breaking into the wave-wake interaction model.

36
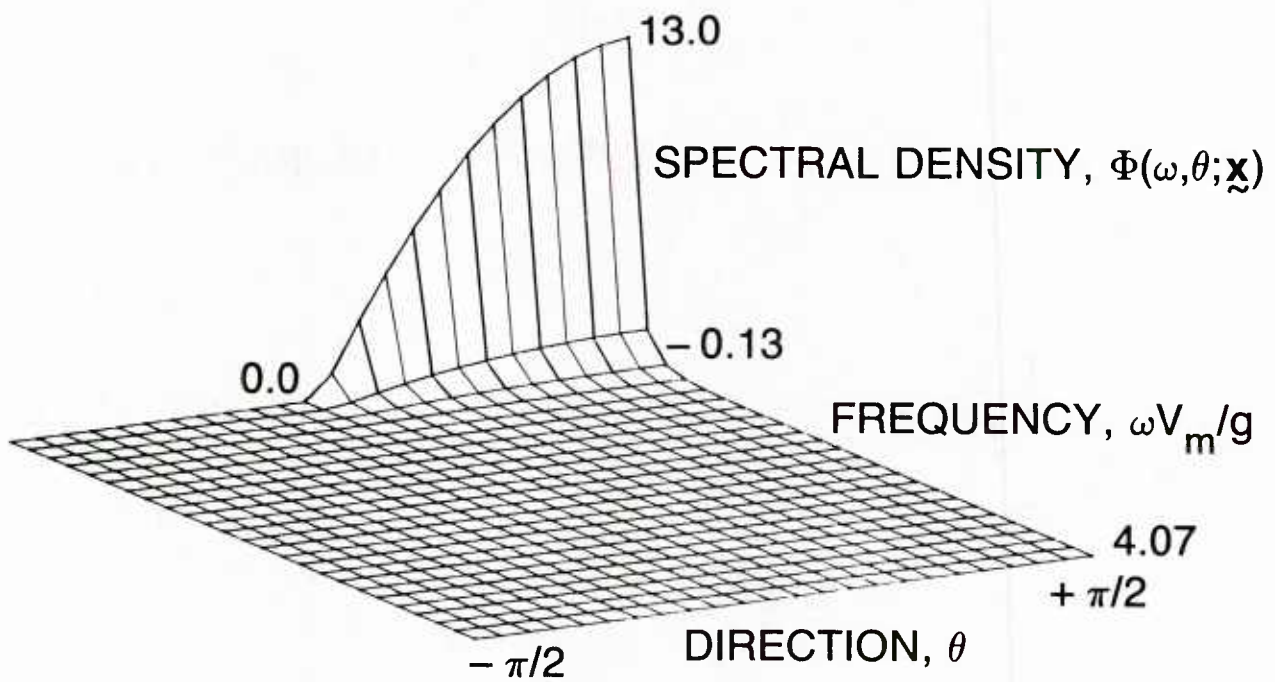
Fig. 16a — Frequency-direction spectral density in the modified wave field. The maximum surface velocity is $V_M = 75$ cm/sec. The ambient spectral density is Pierson-Moskowitz, with a wind speed of 12 m/sec (24 kt). All wave numbers greater than k = 0 in the modified spectrum are shown, for incident wave numbers between k = 0.0005 and 3 cm^{-1}. The waves and current are collinear and unidirectional.

$$y = -24 \text{ m}$$
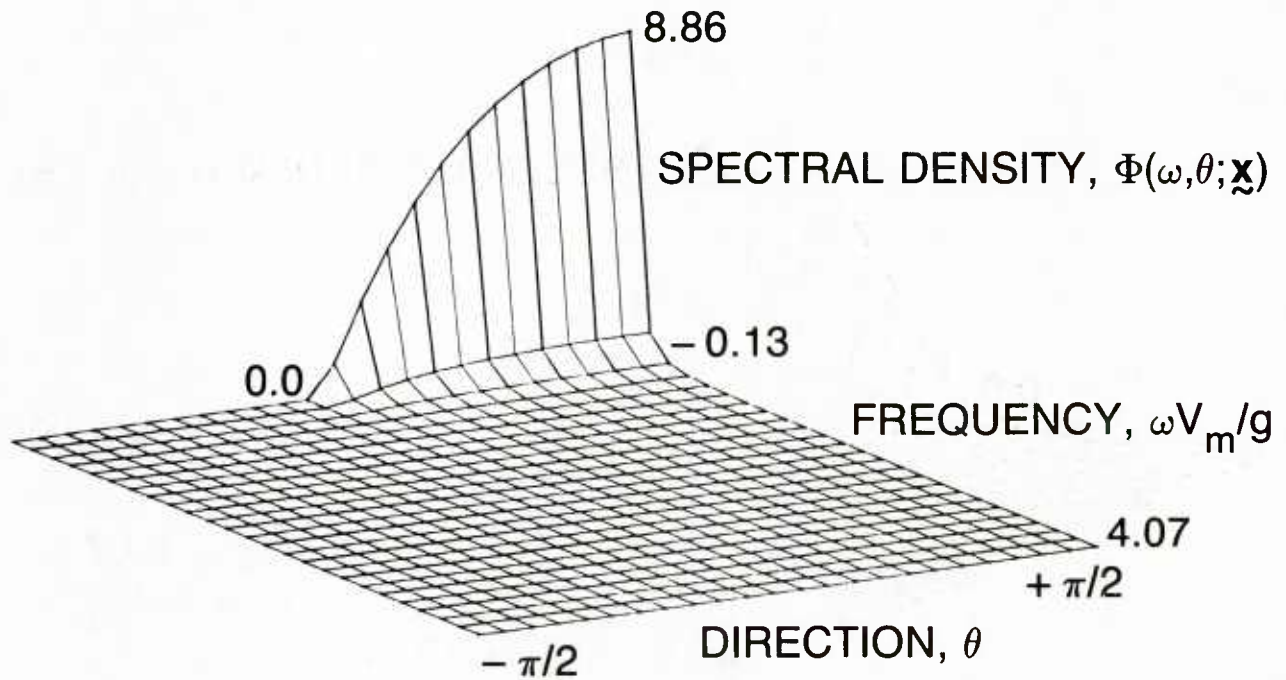
Fig. 16b — Frequency-direction spectral density in the modified wave field. The maximum surface velocity is $V_M = 75$ cm/sec. The ambient spectral density is Pierson-Moskowitz, with a wind speed of 12 m/sec (24 kt). All wave numbers greater than k = 0 in the modified spectrum are shown, for incident wave numbers between k = 0.0005 and 3 cm^{-1}. The waves and current are collinear and unidirectional.

$$y = 0$$
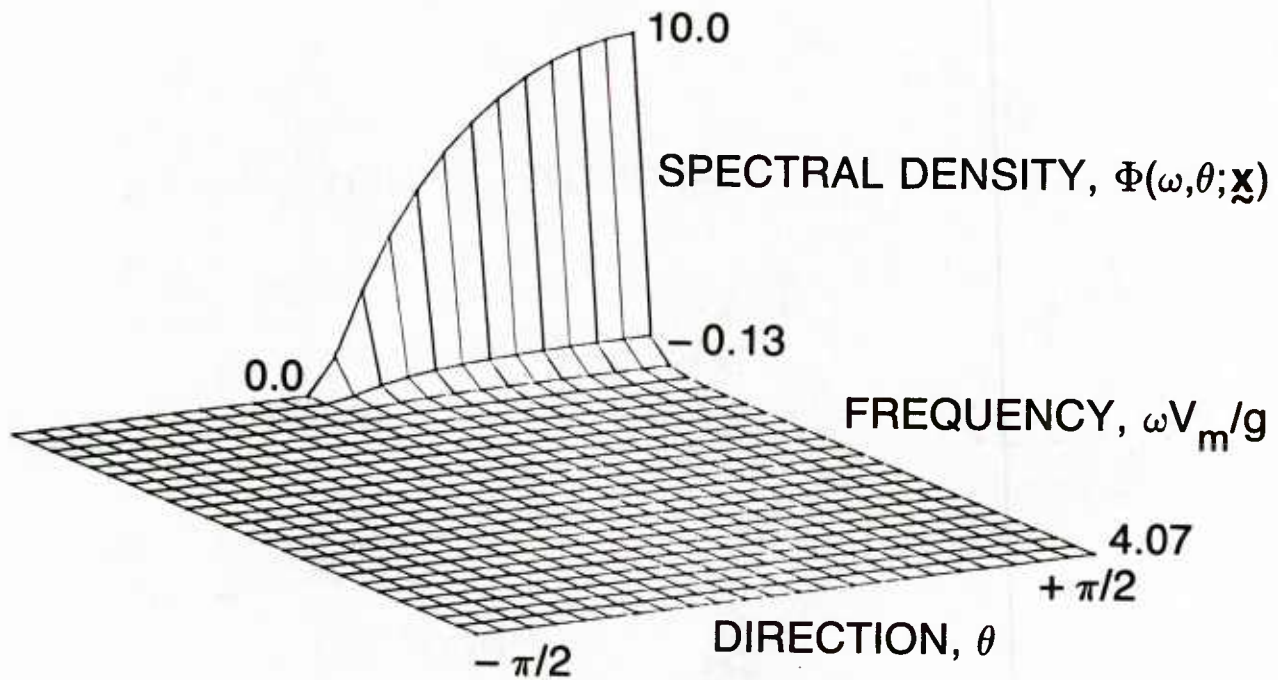
Fig. 16c — Frequency-direction spectral density in the modified wave field. The maximum surface velocity is $V_M = 75$ cm/sec. The ambient spectral density is Pierson-Moskowitz, with a wind speed of 12 m/sec (24 kt). All wave numbers greater than $k = 0$ in the modified spectrum are shown, for incident wave numbers between $k = 0.0005$ and 3 cm^{-1}. The waves and current are collinear and unidirectional.

$$y = +7 \text{ m}$$
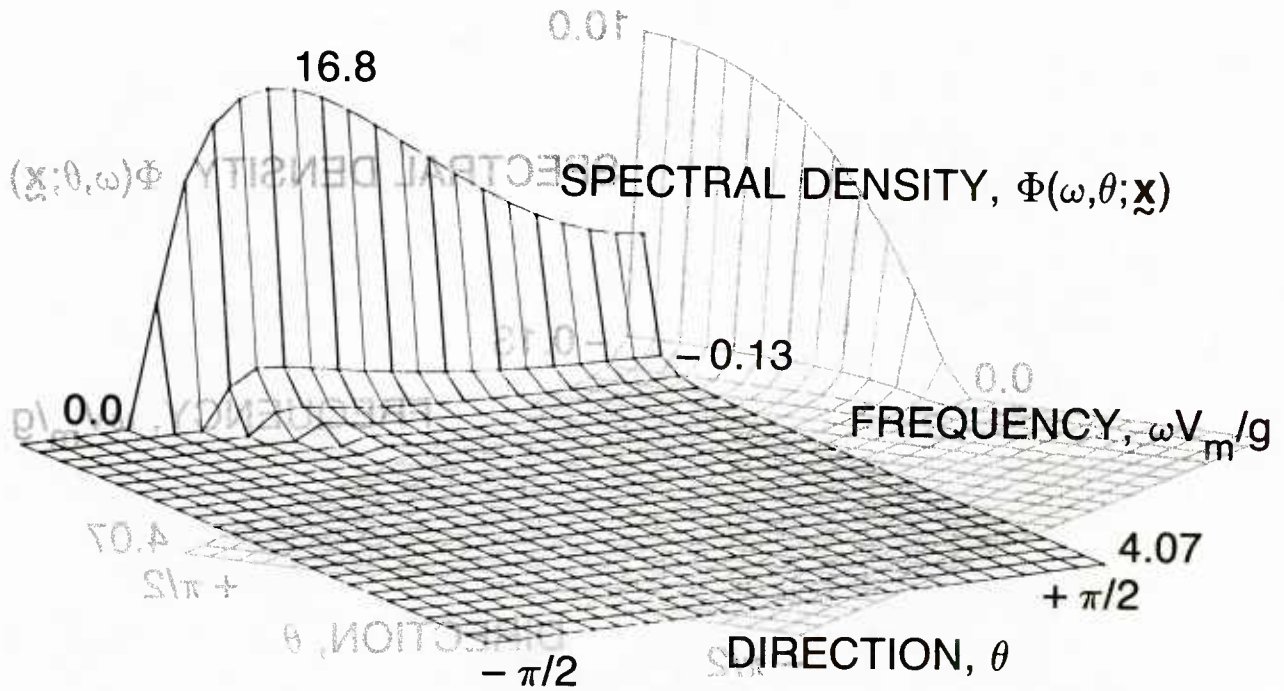
Fig. 17a — Frequency-direction spectral density in the modified wave field. The principal direction of the wave field is normal to the current; other conditions are the same as in Fig. 16.
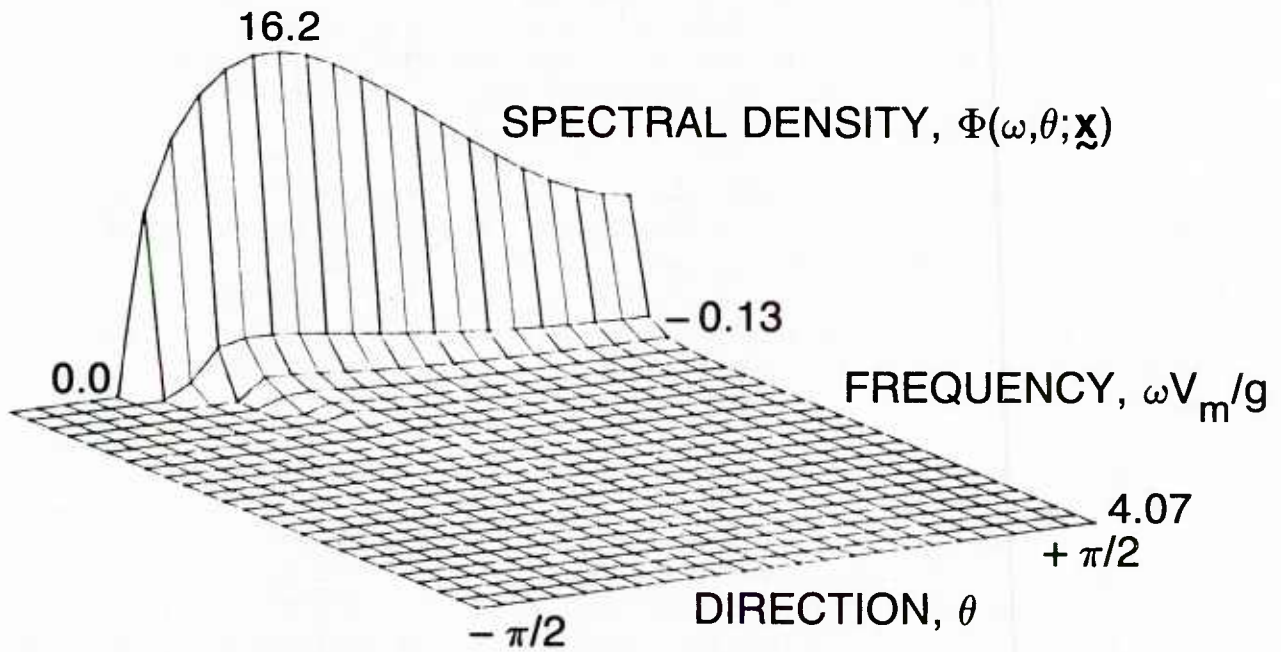
Fig. 17b — Frequency-direction spectral density in the modified wave field. The principal direction of the wave field is normal to the current; other conditions are the same as in Fig. 16.

$$y = +7 \text{ m}$$

SUMMARY

Remote synthetic aperture radar (SAR) images of surface ship wakes often show that the usual wedge-shaped steady Kelvin ship wave pattern with a half-angle of 19.5 degrees is modified such that a bright narrow-v wake image is formed downstream of the ship. The half-angle of this narrow wake has been observed in the SEASAT and DREP experiments to be as small as 3 to 4 degrees, and half-angles of 14 to 16 degrees are common to the SIR-B experiments. These modified Kelvin wakes are usually observed when the ship is traveling in the azimuthal direction of up to 45 degrees relative to the aircraft, spacecraft or satellite which is carrying the radar; that is, in a direction nearly parallel to the flight direction. Then the radar is sensitive to waves which travel in the range direction, i.e. toward or away from the ship's track. These are thought to be ship-generated Bragg waves for the very narrow (3 to 4 degree) wakes.

In contrast to the bright-v wake images there also is a relatively narrow, stem-like dark image along the ship track which often persists for many kilometers downstream. The dark portion of the radar image suggests that this region is relatively smooth and free of short-wavelength scatterers. This region often is described as the turbulent wake or scar of the ship, and the lack of scatterers is ascribed to the interaction of the ship's turbulent wake with the surface wave field. Another suggestion is that the persistence of the dark scar region is due to the redistribution of surfactant materials at and near the water surface as a result of the ship's passage.

A model has been outlined in this paper for characterizing the modification of a random ocean surface wave field by a surface current or wake flow pattern. At the most fundamental level, for a white-noise ambient spectrum, the mean-square surface elevation energy can be computed for a wide range of conditions. More realistic ambient spectral distributions such as Pierson-Moskowitz and that of Phillips (1985) also can be introduced, the results can be subdivided into various wavelength and frequency ranges, and changes in the surface elevations and wave spectra throughout the wave-wake interaction region can be determined.

An important component in the overall wave-current interaction model is the definition of a condition or criterion for the limiting steepness or the onset of wave breaking. A new method for estimating the limiting steepness from the recent experiments of Ramberg and Griffin (1987) and of Ochi and Tsai (1983) is described here. This limiting steepness condition has been employed recently by Huang et al. (1986) in developing an analytical model for oceanic whitecap coverage.

A model for predicting the modification of the Kelvin ship wave pattern by interaction with a surface current field also is described briefly. Not only are the lines of constant phase and the bounds of the Kelvin-v angle modified, but also the wave lengths and, potentially, the wave steepness in the ship wave pattern. The surface wake or current conditions required to produce a modified v angle of 16 degrees are qualitatively in agreement with recent measurements of the surface mean flow pattern in the near wake of a high speed destroyer model.

Recent computations by Swean (1987) to simulate the turbulent wake of a high speed destroyer from model test data have been combined here with the surface wave modification model to predict the interaction of short waves with the surface mean wake flow pattern. The short waves in the 5 to 30 cm wavelength band interact strongly with the wake close to the ship stern where the surface mean flow is approximately 75 cm/sec (1.5 kt) full-scale, but the interaction is greatly diminished when the surface flow decreases to about 10 cm/sec. The latter condition corresponds to a distance of only about 12 ship beams, or 1.5 ship lengths, astern. Thus the downstream extent of the mean turbulent surface wake caused by the ship passage is not sufficient to explain the persistence of the dark surface scar for the observed extent of often many kilometers.

ACKNOWLEDGMENTS

REFERENCES

Banner, M.L. and Fooks, E.H., "On the microwave reflectivity of small-scale breaking water waves," Proceedings of the Royal Society of London, Series A, Vol. 399, 93-109, 1985.

Cooper, A.L. "Interactions between Ocean Surface Waves and Currents," NRL Memorandum Report 5755, April 1986.

Cooper, A.L. and Skop, R.A., "The Turbulent Wake of a Cylindrical Body Traveling Beneath a Free Surface," Proceedings of the Fourth International Conference on Numerical Methods in Laminar and Turbulent Flows, Pineridge Press: Swansea, 659-671, 1985.

Cooper, A.L., Griffin, O.M. and Wang, H.T. "Ocean Wave Modifications by a Surface Current Field," COASTAL HYDRODYNAMICS, ASCE: New York, 479-492, June 1987.

Crapper, G.D., INTRODUCTION TO WATER WAVES, Ellis Horwood Ltd.: Chichester; Chap. 5, 1984.

Griffin, O.M., "Ship Wave Modification by a Surface Current Field," Journal of Ship Research, Vol. 32, in press, 1988.

Hammond, R.R., Buntzen, R.R. and Floren, E.E., "Using Ship Wake Patterns to Evaluate SAR Ocean Wave Imaging Mechanisms," Naval Ocean Systems Center Technical Report 978, 1985.

Hedges, T.S., Anastasion, K. and Grabriel, D., "Interaction of Random Waves and Currents," Journal of Waterway, Port, Coastal and Ocean Engineering, ASCE, Vol. 111, No. 2, 275-288, 1985.

Huang, N.E., Bliven, L.F., Long, S.R. and Tung, C.C., "An Analytical Model for Oceanic Whitecap Coverage," Journal of Physical Oceanography, Vol. 16, 1597-1604, 1986.

James, E.C., Collins, J.I., Wagner, P.A. and Tayfun, M.A., "Ocean Wave Spectrum Modifications by Spatially Varying Currents and Bottom Topography," Tetra Tech Report No. TC-493-1, 1977.

Kaiser, J.A.C., Ramberg, S.E., Peltzer, R.D., Andrews, M.D., and Garrett, W.D., "WAKEX 86," NRL Memorandum Report, in press, 1988.

Keramidas, G.A. and Bauman, W., "FFSW: A Computer Code for Far Field Ship Wave Calculations," NRL Memorandum Report 6007, 1987.

Keramidas, G.A., Griffin, O.M., Swean, T.F. Jr., and Stewart, M.B., "An Integrated Software System for Ship Wake Hydrodynamic Modelling," Ocean Engineering, to appear, 1988.

Kjeldsen S.P., and Myrhaug D., "Kinematics and Dynamics of Breaking Waves," Norwegian Hydrodynamics Laboratory Report STF60A78100, 1978.

Lighthill, M.J., *WAVES IN FLUIDS*, Cambridge University Press; Chap. 4 and Epilogue, 1979.

Lindenmuth, W.T., "Private communication: Data from the Model 5415 experiment at the David Taylor Research Center," 1986.

Longuet-Higgins, M.S., "The generation of capillary waves by steep gravity waves," Journal of Fluid Mechanics, Vol. 16, 138-159, 1963.

Longuet-Higgins, M.S., "On wave breaking and the equilibrium spectrum of wind-generated waves," Proceedings of the Royal Society, Series A, Vol. 310, 151-159, 1969.

Longuet-Higgins, M.S., "Integral Properties of Periodic Gravity Waves of Finite Amplitude," Proceedings of the Royal Society of London, Series A, Vol. 342, 157-174, 1975.

Longuet-Higgins, M.S. and Stewart, R.W., "The Changes in Amplitude of Short Gravity Waves on Steady Non-Uniform Currents," Journal of Fluid Mechanics, Vol. 10, 529-549, 1961.

Longuet-Higgins, M.S. and Stewart, R.W., "Radiation Stress in Waves, a Physical Description with Applications," Deep Sea Research, Vol. 11, 529-562, 1964.

Lyden, J.D., Lysenga, D.R., Schuchman, R.A. and Kasischke, E.S., "Analysis of Narrow Ship Wakes in Georgia Strait SAR Data," Environmental Research Institute of Michigan (ERIM) Topic Report 155900-20-T, 1985.

Meadows, G.A., private communication, 1987.

Melville, W.K., "The instability and breaking of deep-water waves," Journal of Fluid Mechanics, Vol. 115, 165-185, 1982.

Melville, W.K. and Rapp, R.J., "Momentum flux in breaking waves," Nature, Vol. 317, 514-516, 1985.

Munk, W.H., Scully-Power, P. and Zachariasen, F., "THE BAKERIAN LECTURE 1986 Ships from Space," Proceedings of the Royal Society of London, Series A, Vol. 412, 231-254, 1987.

Nath, J.H., and Ramsey, F.L., "Probability distributions of breaking wave heights emphasizing the utilization of the JONSWAP spectrum," Journal of Physical Oceanography, Vol. 6, 316-323, 1976.

Newman, J.N., *MARINE HYDRODYNAMICS,* MIT Press: Cambridge, Chap. 6, 1977.

Noblesse, F., "A Slender Ship Theory of Wave Resistance," Journal of Ship Research, Vol. 27, 13-33, 1983.

Ochi, M. K. and Tsai, C.-H., "Prediction of Occurrence of Breaking Waves in Deep Water," Journal of Physical Oceanography, Vol. 13, 2008—2019, 1983.

Peregrine, D.H., "A Ship's Waves and Its Wake," Journal of Fluid Mechanics, Vol. 49, 353-360, 1971.

Peregrine, D.H., "Interactions of Water Waves and Currents," Advances in Applied Mechanics, Vol. 16, 9-117, 1976.

Peregrine, D.H., and Thomas, G.P., "Finite-Amplitude Deep Water Waves on Currents," Philosophical Transactions of the Royal Society of London, Series A, Vol. 292, 371-390, 1979.

Phillips, O.M., "Spectral and statistical properties of the equilibrium range in wind-generated gravity waves," Journal of Fluid Mechanics, Vol. 156, 505-531, 1985.

Ramberg, S.E. and Griffin, O.M., "Laboratory Studies of Steep and Breaking Deep Water Waves," Journal of Waterway, Port, Coastal and Ocean Engineering, ASCE, Vol. 113, No. 5, 493-506, 1987.

Reed, A.M., private communication, 1986.

Sakai, T., Koseki, M. and Iwagaki, Y., "Irregular Wave Refraction Due to Current," Journal of Hydraulic Engineering, ASCE, Vol. 109, No. 9, 1203-1215, 1983.

Savitsky, D.M., "Interaction Between Gravity Waves and Finite Flow Fields," Eighth Symposium on Naval Hydrodynamics (Proceedings), Office of Naval Research: Arlington, VA, 389-447, 1970.

Skop, R.A., "The Hydrodynamic Wake of a Surface Ship: Theoretical Foundations," NRL Report No. 8833, 1984.

Skop, R.A., private communication, 1987.

Skop, R.A. and Liepold, Y., "Modification of Directional Wave Number Spectra by Surface Currents," Ocean Engineering, in press, 1988.

Srokosz, M.A., "On the Probability of Wave Breaking in Deep Water," Journal of Physical Oceanography, Vol. 16, 382-385, 1986.

Su, M.-Y., Bergin, M., Marler, P., and Myrick, R., "Experiments on nonlinear instabilities and evolution of steep gravity-wave trains," Journal of Fluid Mechanics, Vol. 124, 45-71, 1982.

Swean, T.F., Jr., "Numerical Simulations of the Wake Downstream of a Twin-Screw Destroyer Model," NRL Memorandum Report 6131, 1987.

Tayfun, M.A., Dalrymple R.A., and Yang, C.Y., "Random Wave—Current Interactions in Water of Varying Depth," Ocean Engineering, Vol. 3, 403-420, 1976.

Ursell, F., "On Kelvin's ship wave pattern," Journal of Fluid Mechanics, Vol. 8, 418-432, 1960.

Wang, H.T., "Temporal and Spatial Simulations of Random Ocean Waves," Proceedings of the Fourth Offshore Mechanics and Arctic Engineering (OMAE) Symposium, ASME, Vol. I, 72-80, 1985.

Wang, H.T., and Rogers, J.C.W., "Spectral Comparisons of Ocean Waves and Kelvin Ship Waves," Proceedings of the Seventh Offshore Mechanics and Arctic Engineering (OMAE) Symposium, ASME: New York, Vol. II, 253-261, 1988.

Witting, J.M. and Vaglio-Laurin, R., "Mechanisms and Models of Narrow-V Wakes," ORI Inc. Technical Report 2529, October 1985.

APPENDIX

The FSWCI Computer Code

The FSWCI computer code has been developed to provide a computation of the modified surface amplitude field in deep water that results from the interaction between a surface shear current or wake flow pattern and an ambient wave field. The basic formulation was given by James et al. (1977) and is based upon conservation of the wave action, or the ratio of the wave energy density and the local, or intrinsic, wave frequency. The original formulation of James et al. was based upon a white noise or "top hat" constant ambient wave spectral density; in the present FSWCI code the white noise spectrum is replaced by a more general Pierson-Moskowitz spectral density. Other spectra in common usage can be introduced into the model with equal facility. The present version of the program is based on a frequency-direction formulation. A wave number-direction formulation including radar cross-section (RCS) predictions in the perturbed surface plane is presently under development for implementation into a related computer code (Skop and Leipold, 1988).

The modified surface wave field can be computed over an arbitrary range of ambient wave numbers using up to 51×51 grid points in the surface (x,y) plane. The local modified frequency-direction spectral density can be computed using up to 25×24 grid points, respectively. The program is menu-driven and user-friendly, and is configured to run on the Hewlett-Packard 9000 Series of computers (presently Models 550 and 320). A listing of the FSWCI computer code follows. Further information is available from the first author.

47

```
**                                                                      **
**********************************************************************
**                                                                      **
      PROGRAM FSWCI
**                                                                      **
**********************************************************************
**                                                                      **
      COMMON /INP/ GEE,UM,Y0,Y1,W1,PI,YM,WD,DY,WL,XS(100),YS(100),
     .             U(100),NX,NY,PSIW,UW,NW,NT,DELTH,AKL,NREC,NS(10),
     .             TITLE,SPEC(10)
      COMMON /OUT1/ DELW(99),THET(99),THETA(99),WS(99),THIR(99),THL(99)
      COMMON /OUT2/ ZETA(101,101),ZETA2(101,101),XX(101),YY(101)
      COMMON /OUT3/ F(99,99),ETA(99,99),AK(99,99),PH(99,99),F2(99,99)
**
      CHARACTER*1 ANS
      CHARACTER*40 SPEC
      CHARACTER*80 TITLE
**
   10 CALL INPUT
**
*****  Compute the spectral density at each point along the Y-axis.
**
      CALL SPECMOD
**
      CALL CLEAR_DISPLAY
      WRITE(*,'(5(/),5X,
     .    "*********************************************************",
     ./,5X,"**  Would you like to run another case? (y,n): ",$)')
      READ(*,'(A1)') ANS
      IF (ANS .EQ. 'Y' .OR. ANS .EQ. 'y') GOTO 10
**
      STOP
      END
**                                                                      **
**********************************************************************
**                                                                      **
      SUBROUTINE INPUT
**                                                                      **
**********************************************************************
**                                                                      **
**  Dimensional form of input, defines KL, WL, etc.,                    **
**      to be used with REFRACT and SPECMOD.                            **
**                                                                      **
**  INPUT requires dimensional values of K1, K2, and KL, along with     **
**      dimensional value of UM in cm/sec, UW in knots, and all K       **
**      values in cm-1.                                                 **
**                                                                      **
**********************************************************************
**                                                                      **
      COMMON /INP/ GEE,UM,Y0,Y1,W1,PI,YM,WD,DY,WL,XS(100),YS(100),
```

48

```fortran
     .                   U(100),NX,NY,PSIW,UW,NW,NT,DELTH,AKL,NREC,NS(10),
     .                   TITLE,SPEC(10)
**
      CHARACTER*1 ANS
      CHARACTER*40 NFILE,SPEC,NSPEC
      CHARACTER*80 TITLE,NTITLE
**
      PI = 2.0*ASIN(1.0)
      GEE = 980.0
**
      CALL CLEAR_DISPLAY
      WRITE(*,'(5(/),5X,
     .        "****************************************************",
     ./,5X,"**                    PROGRAM REFRACT                **",
     ./,5X,"****************************************************")')
      CALL PAUSE_SEC(5)
**
      CALL CLEAR_DISPLAY
      WRITE(*,'(////,
     ./,5X,"****************************************************",
     ./,5X,"**  Would you like to read an input file? (y/n): ",$)')
      READ(*,'(A1)') ANS
      IF (ANS .NE. 'Y' .AND. ANS .NE. 'y') GOTO 10
**
    5 WRITE(*,'(5X,
     .        "****************************************************",
     ./,5X,"**  Enter the name of the input file: ",$)')
      READ(*,'(A40)') NFILE
      OPEN(UNIT=40,FILE=NFILE,FORM='UNFORMATTED',STATUS='OLD',ERR=5)
      READ(40) TITLE,AKL,AK1,AK2,UW,PSIW,UM,U0,Y0,Y1,NX,NY,NY0,NY1,
     .          NW,NT,NREC,(NS(N),N=1,NREC),(SPEC(NN),NN=1,NREC)
      CLOSE(UNIT = 40)
      WRITE(*,'(5X,
     .        "****************************************************",
     ./,5X,"**  Would you like to view or change any of the data? ",$)')
      READ(*,'(A1)') ANS
      IF (ANS .NE. 'Y' .AND. ANS .NE .'y') GOTO 20
**
   10 CALL CLEAR_DISPLAY
      WRITE(*,1010) TITLE
 1010 FORMAT(////,
     ./,5X,"****************************************************",
     ./,5X,"**  Enter the title of the output files.  TITLE =    **",
     ./,A80,
     ./,5X,"**   ENTER  TITLE: ",$)
      READ(*,'(A80)') NTITLE
      IF (NTITLE .NE. '/') TITLE = NTITLE
**
      WRITE(*,1020) AKL
 1020 FORMAT(////,
```

```fortran
      ./,5X,"****************************************************",
      ./,5X,"**  Enter the minimum wave number in cm-1 for files  **",
      ./,5X,"**   Specden, Surf2, and Surface.  AKL = ",F10.5,3X, "**",
      ./,5X,"**  ENTER  AKL: ",$)
      READ(*,*) AKL
**
      WRITE(*,1030) AK1, AK2
 1030 FORMAT(////,
      ./,5X,"****************************************************",
      ./,5X,"**  Enter the minimum and the maximum wave numbers in **",
      ./,5X,"**   cm-1 for the free stream spectrum (ambient).     **",
      ./,5X,"**   AK1, AK2 = ",2F10.5,18X,                          "**",
      ./,5X,"**  ENTER  AK1, AK2: ",$)
      READ(*,*) AK1,AK2
*
      UKNOTS = UW/51.4
      WRITE(*,1040) UKNOTS
 1040 FORMAT(////,
      ./,5X,"****************************************************",
      ./,5X,"**  Enter wind velocity in knots.  UW = ",F10.5,4X,  "**",
      ./,5X,"**  ENTER  UW: ",$)
      READ(*,*) UKNOTS
      UW = UKNOTS*51.4
**
      PANGLE = PSIW*180.0/PI
      WRITE(*,1050) PANGLE
 1050 FORMAT(////,
      ./,5X,"****************************************************",
      ./,5X,"**  Enter the wind direction in degrees.            **",
      ./,5X,"**    PSIW = ",F10.5,32X,                            "**",
      ./,5X,"**  ENTER  PSIW: ",$)
      READ(*,*) PANGLE
      PSIW = PANGLE*PI/180.0
**
      WRITE(*,1060) UM
 1060 FORMAT(////,
      ./,5X,"****************************************************",
      ./,5X,"**  Enter the maximum current velocity in cm/sec    **",
      ./,5X,"**   (parabolic).  UM = ",F10.5,20X,                 "**",
      ./,5X,"**  ENTER  UM: ",$)
      READ(*,*) UM
**
      WRITE(*,1070) U0
 1070 FORMAT(////,
      ./,5X,"****************************************************",
      ./,5X,"**  Enter the velocity of the constant stream in    **",
      ./,5X,"**   cm/sec.  U0 = ",F10.5,25X,                      "**",
      ./,5X,"**  ENTER  U0: ",$)
      READ(*,*) U0
**
```

50

```
      WRITE(*,1080) Y0, Y1
 1080 FORMAT(////,
     ./,5X,"**************************************************",
     ./,5X,"**   Enter the boundaries of the complete stream in   **",
     ./,5X,"**    meters.  Y0, Y1 = ",2F10.5,11X,              "**",
     ./,5X,"**   ENTER  Y0, Y1: ",$)
      READ(*,*) Y0,Y1
**
      WRITE(*,1090) NX, NY
 1090 FORMAT(////,
     ./,5X,"**************************************************",
     ./,5X,"**   Enter the number of points in the X and the Y   **",
     ./,5X,"**    directions.  NX, NY = ",2I5,17X,              "**",
     ./,5X,"**   ENTER  NX, NY: ",$)
      READ(*,*) NX,NY
**
      WRITE(*,1100) NY0, NY1
 1100 FORMAT(////,
     ./,5X,"**************************************************",
     ./,5X,"**   Enter the points which mark the boundaries of the **",
     ./,5X,"**    parabolic current flow.  NY0, NY1 = ",2I5,3X,  "**",
     ./,5X,"**   ENTER  NY0, NY1: ",$)
      READ(*,*) NY0,NY1
**
      WRITE(*,1110) NW, NT
 1110 FORMAT(////,
     ./,5X,"**************************************************",
     ./,5X,"**   Enter the number of points for the Omega and    **",
     ./,5X,"**    Theta grid (spectral density). NW, NT = ",2I4,1X"**",
     ./,5X,"**   ENTER  NW, NT: ",$)
      READ(*,*) NW,NT
**
      WRITE(*,1120) NREC
 1120 FORMAT(////,
     ./,5X,"**************************************************",
     ./,5X,"**   Enter the number of spectral density files you  **",
     ./,5X,"**    wish to create.  NREC = "I4"                  **",
     ./,5X,"**   ENTER  NREC: ",$)
      READ(*,*) NREC
**
      WRITE(*,1130) (NS(N),N=1,10),NREC
 1130 FORMAT(////,
     ./,5X,"**************************************************",
     ./,5X,"**   Enter each Y-location at which spectral density  **",
     ./,5X,"**    information is desired.                       **",
     ./,5X,"**   NS = ",10(I3),15X,                             "**",
     ./,5X,"**   ENTER all "I4" values of NS: ",$)
      READ(*,*) (NS(N),N=1,NREC)
**
      WRITE(*,1140)
```

51

```fortran
 1140 FORMAT(////,
     ./,5X,"****************************************************",
     ./,5X,"**   Enter the file names for the spectral density   **",
     ./,5X,"**   output files.                                    **",
     ./,5X,"****************************************************")
      DO NN = 1,NREC
        WRITE(*,1150) NN, SPEC(NN)
 1150    FORMAT(/,
     .   5X,"**                                                   **",
     ./,5X,"**   File # ",I2," File Name : ",A40,
     ./,5X,"**   ENTER new filename -OR- [/] :",$)
        READ(*,'(A40)') NSPEC
        IF (NSPEC .NE. '/') SPEC(NN) = NSPEC
      END DO
*
      WRITE(*,1160)
 1160 FORMAT(////,
     ./,5X,"****************************************************",
     ./,5X,"**   Would you like to change any of the data? (y/n): ",$)
      READ(*,'(A1)') ANS
      IF (ANS .EQ. 'Y' .OR. ANS .EQ. 'y') GOTO 10
**
      CALL CLEAR_DISPLAY
      WRITE(*,'(5(/),5X,
     .   "****************************************************",
     ./,5X,"**   Do you wish to save the data in an input file for **",
     ./,5X,"**    future use? (y/n): ",$)')
      READ(*,'(A1)') ANS
**
      IF (ANS .EQ. 'Y' .OR. ANS .EQ. 'y')  THEN
        WRITE(*,'(5X,
     .   "****************************************************",
     ./,5X,"**   Enter the name of the input file: ",$)')
        READ(*,'(A40)') NFILE
        OPEN(UNIT=40,FILE=NFILE,FORM='UNFORMATTED')
        WRITE(40) TITLE,AKL,AK1,AK2,UW,PSIW,UM,U0,Y0,Y1,NX,NY,NY0,NY1,
     .            NW,NT,NREC,(NS(N),N=1,NREC),(SPEC(NN),NN=1,NREC)
        CLOSE(UNIT = 40)
      END IF
**
   20 UN = UM - U0
      DY = (Y1 - Y0)/FLOAT(NY - 1)
**
*****  For a square realization plane.
**
      DO I = 1,NY
        YS(I) = Y0 + DY*(I - 1)
        XS(I) = DY*(I - 1)
      END DO
**
```

```
            DO I = 1,NY
              IF (I .LE. NY0 .OR. I .GE. NY1)   THEN
                U(I) = U0
              ELSE
                U(I) = (YS(I) - YS(NY0))*(YS(I) - YS(NY1))*(-4.0*UN/(YS(NY1)
                       - YS(NY0))**2) + U0
              END IF
            END DO
**
            W1 = SQRT(GEE*AK1)*UM/GEE
            W2 = SQRT(GEE*AK2)*UM/GEE
            DELTH = PI/NT
            YM = 0.5*(Y1 + Y0)
            WD = 0.5*(W2 - W1)
            WL = SQRT(GEE*AKL)*UM/GEE
**
            RETURN
            END
**                                                                    **
**********************************************************************************
**                                                                    **
            SUBROUTINE SPECMOD
**                                                                    **
**********************************************************************************
**                                                                    **
**   This version of SPECMOD provides a realization for a varying     **
**      current.                                                      **
**   NOTE:   XL**2 has been removed from the line " 821 F(II,J)=... "  **
**           the old instruction has been commented out.  This needs  **
**           to be done to the other &INTF@.                          **
**                                                                    **
**   This version includes a Pierson-Moskowitz spectral density and   **
**      has taken into consideration both the incoming and outgoing   **
**      waves by introducing additional terms to ZETA and an additional **
**      random phase PH2.                                             **
**                                                                    **
**********************************************************************************
**                                                                    **
            COMMON /INP/ GEE,UM,Y0,Y1,W1,PI,YM,WD,DY,WL,XS(100),YS(100),
           .             U(100),NX,NY,PSIW,UW,NW,NT,DELTH,AKL,NREC,NS(10),
           .             TITLE,SPEC(10)
            COMMON /OUT1/ DELW(99),THET(99),THETA(99),WS(99),THIR(99),THL(99)
            COMMON /OUT2/ ZETA(101,101),ZETA2(101,101),XX(101),YY(101)
            COMMON /OUT3/ F(99,99),ETA(99,99),AK(99,99),PH(99,99),F2(99,99)
**
            CHARACTER*40 SPEC
            CHARACTER*80 TITLE
**
            CALL CLEAR_DISPLAY
**
```

53

```
        OPEN(UNIT=66,FILE='refract.out')
**
*****  Here we want to expand the Omega and Theta grid.
**
**
        DO  K = 1,NW
          DELW(K) = 2.0*WD/NW
          WS(K) = W1 + 0.5*DELW(K)*(2*K - 1)
        END DO
**
        DO II = 1,NT+1
          THET(II) = -0.5*PI + (II - 1)*DELTH
        END DO
**
        DO II = 1,NT
          THETA(II) = 0.5*(THET(II+1) + THET(II))
        END DO
**
*****  This section calculates the Fourier coefficients of the
*****    frequency direction spectral density and the coefficients
*****    of the surface elevation field ...... F(W(J),THET(I)).
**
        TFACTOR = GEE/UM
        WRITE(*,'(//////)')
        DO I = 1,NY
        WRITE(*,'(">>>>>   Computing. Please wait. I =",I3)') I
        XL = U(I)/UM
        XLT = 1.0/XL
        DO J = 1,NW
          W = WS(J)
          EEE = 0.5*(1.0 + 2.0*W - SQRT(1.0 + 4.0*W))/(W*W)
          IF (W .LT. 0.1) EEE = 1.0 - 2.0*W + 5.0*W*W - 14.0*W*W*W +
                                42.0*W**4 - 132.0*W**5
          TIR = ASIN(EEE)
          AB = -XLT/W
          IF (W .LT. XLT) AB = -1.0
          TB = -0.5*PI
          IF (W .GT. XLT) TB = ASIN(AB)
          TM = 0.5*(TIR + TB)
          TD = 0.5*(TIR - TB)
          UNIT = 1.0
          IF (W .LT. WL) UNIT = -1.0
          TL = UNIT*0.5*PI
          STHL = XLT*(W - WL)/W**2
          IF (ABS(STHL) .LE. 1.0) TL = ASIN(STHL)
          THL(K) = TL
          DO II = 1,NT
            ETA(II,J) = WS(J)*SIN(THETA(II))
            BR = 4.0*XL*ETA(II,J)
            THEX = ASIN(-1.0/(1.0 + XL*WS(J))**2)
```

54

```fortran
                IF (SIN(THEX) .GT. (-1.0/(4.0*XL*WS(J)))) GOTO 823
                IF (BR .LT. -1.0) GOTO 820
                GOTO 821
  823           IF (THETA(II) .LT. THEX) GOTO 820
                GOTO 821
  820           F(II,J) = 0.0
                GOTO 822
  821           ETAIIJ = 2.0*XL*ETA(II,J)
                SQETA = SQRT(1.0 + 4.0*XL*ETA(II,J))
                FIIJ = ((SQETA - 1.0)/ETAIIJ)**4/SQETA*DELW(J)*WS(J)*DELTH
**
*****   These next instructions will insert the Pierson-Moskowitz
*****    incoming frequency function.
*****      S(W)/W = 0.0081(UM)**6/(G**4*W**6)*EXP(-0.74(UM/(UW*W))**4)
*****   where UW=wind velocity in cm/sec and must be defined.
**
                F(II,J) = FIIJ*0.0081*UM**6/((WS(J)**6)*(GEE**4))*
                          EXP(-0.74*(UM/(UW*WS(J)))**4)
**
*****   Insert        G(TH)=(COS(NU(THINF-PSIW))**2
*****   where NU is a parameter of the P/M model and PSIW is the angle
*****   between the wind and the wake centerline and THINF is the
*****   direction in the initial plane for WJ and THI.
*****   We need to insure that ABS(NU*THW) < PI/2.0
**
                IF (F(II,J) .NE. 0.0)   THEN
                   ENU = 1.0
                   ETAIIJ = 2.0*XL*ETA(II,J)
                   SQETA = SQRT(1.0 + 4.0*XL*ETA(II,J))
                   SNTHO = (1.0 + ETAIIJ - SQETA)/(XL*ETAIIJ*WS(J))
                   IF (ABS(SNTHO) .GE. 1.0)   THEN
                      SNTHO = (1.0 - ETAIIJ +
                               5.0*(XL*ETA(II,J))**2)*SIN(THETA(II))
                   END IF
                   THINF = ASIN(SNTHO)
c                  THW = THINF - PSIW
                   ENUTH = THINF - PSIW
c                  THW2 = PI - THINF + PSIW
                   ENUTH2 = PI - THINF + PSIW
                   IF (ABS(ENUTH2) .GE. 0.5*PI)   THEN
                      F2(II,J) = 0.0
                   ELSE
                      F2(II,J) = F(II,J)*(COS(ENUTH2))**2
                   END IF
                   IF (ABS(ENUTH) .GE. 0.5*PI)   THEN
                      F(II,J) = 0.0
                   ELSE
                      F(II,J) = F(II,J)*(COS(ENUTH))**2
                   END IF
                END IF
```

55

```
**
  822      F(II,J) = SQRT(2.0*F(II,J))*TFACTOR
           F2(II,J) = SQRT(2.0*F2(II,J))*TFACTOR
**
*****  The nondimensional wavenumber, KIJ is now computed AK(I,J)
*****     the dimensional K is produced by multiplying by UM**2/G
**
           ETAIJ = 4.0*XL*ETA(II,J)
           IF (ETAIJ .LT. -1.0)   THEN
             AK(II,J) = 0.0
             F(II,J) = 0.0
             F2(II,J) = 0.0
           ELSE
             ETAIIJ = 2.0*XL*ETA(II,J)
             SQETA = SQRT(1.0 + 4.0*XL*ETA(II,J))
             AK(II,J) = (WS(J)*(SQETA - 1.0)/ETAIIJ)**2
           END IF
           AKIJ = AK(II,J)
           IF (AKIJ .LT. AKL*UM/TFACTOR)   THEN
             AK(II,J) = 0.0
             F(II,J) = 0.0
             F2(II,J) = 0.0
           END IF
         END DO
         IF (I .EQ. NS(1))   THEN
           WRITE(66,'(4X,12E10.5)') (F(K,J),K=1,12)
           WRITE(66,'(4X,12E10.5)') (F(K,J),K=13,24)
         END IF
       END DO
**
       IF (I .EQ. NS(1))   THEN
         DO J = 1,25
           WRITE(66,'(4X,12E10.5)') (AK(K,J),K=1,12)
           WRITE(66,'(4X,12E10.5)') (AK(K,J),K=13,24)
         END DO
       END IF
**
       CALL SPECTRA_FILE(I)
**
*****  Initialize ZETA(II,J).
**
       II = I
       DO J = 1,NY
         ZETA(J,II) = 0.0
         ZETA2(J,II) = 0.0
       END DO
**
*****  Random phase.
**
       JT = 1
```

56

```
        DO IR = 1,NT
          DO JR = 1,NW
            PH(IR,JR) = URAND(JT)*2.0*PI
          END DO
        END DO
**
*****   Define physical position.
**
        COEFF = 100.0*TFACTOR/UM
        XX(I) = COEFF*XS(I)
        DO JJ = 1,NY
          YY(JJ) = COEFF*YS(JJ)
          DO JT = 1,NW
**
*****   Reflection boundary THETA = THIR.
**
            WSJT =  SQRT(1.0 + 4.0*WS(JT)) - 1.0
            THIR(JT) = ASIN((WSJT/(2.0*WS(JT)*(1.0 - XL) + XL*WSJT))**2)
            DO IT = 1,NT
**
*****   These next lines are needed to control angles to be less then
*****       1000*PI as requred.
**
              THP = AK(IT,JT)*(XX(II)*SIN(THETA(IT)) +
     .              YY(JJ)*COS(THETA(IT))) + PH(IT,JT)
              THM = AK(IT,JT)*(XX(II)*SIN(THETA(IT)) -
     .              YY(JJ)*COS(THETA(IT))) + PH(IT,JT)
              IF (ABS(THP) .GE. 1000.0*PI)   THEN
                III = THP/(2.0*PI)
                THP = THP - III*2.0*PI
              END IF
              IF (ABS(THM) .GE. 1000.0*PI)   THEN
                III = THM/(2.0*PI)
                THM = THM - III*(2.0*PI)
              END IF
              Y = YS(JJ)
              THETAIT = THETA(IT)
              THIRJT = THIR(JT)
              IF (THETAIT .LT. THIRJT .OR. Y .GE. YM)   THEN
                ZETA(JJ,II) = ZETA(JJ,II) + F(IT,JT)*COS(THP)
              ELSE
                ZETA(JJ,II) = ZETA(JJ,II) +
     .                          F(IT,JT)*(COS(THP) + COS(THM))
              END IF
              THETAIT = THETA(IT)
              THIRJT = THIR(JT)
              IF (THETAIT .LT. THIRJT)   THEN
                ZETA2(JJ,II) = ZETA2(JJ,II) +
     .                          F(IT,JT)*(COS(THP)+COS(THM))
              ELSE
```

57

```
                         ZETA2(JJ,II) = ZETA2(JJ,II) +
                                    F(IT,JT)*COS(THP) + F2(IT,JT)*COS(THM)
                   END IF
                 END DO
               END DO
            END DO
            END DO
            CALL PLOT_FILE
**
            CLOSE(UNIT = 66)
**
            RETURN
            END
**                                                                          **
****************************************************************************
**                                                                          **
            SUBROUTINE OUTPUT
**                                                                          **
****************************************************************************
**                                                                          **
**    This subroutine outputs the data files.                               **
**                                                                          **
****************************************************************************
**                                                                          **
            COMMON /INP/ GEE,UM,Y0,Y1,W1,PI,YM,WD,DY,WL,XS(100),YS(100),
        .                U(100),NX,NY,PSIW,UW,NW,NT,DELTH,AKL,NREC,NS(10),
        .                TITLE,SPEC(10)
            COMMON /OUT1/ DELW(99),THET(99),THETA(99),WS(99),THIR(99),THL(99)
            COMMON /OUT2/ ZETA(101,101),ZETA2(101,101),XX(101),YY(101)
            COMMON /OUT3/ F(99,99),ETA(99,99),AK(99,99),PH(99,99),F2(99,99)
**
            CHARACTER*40 SPEC
            CHARACTER*80 TITLE
**
*****   Write the output files.
**
            ENTRY SPECTRA_FILE(I)
            NDIM = 1
**
            DO NN = 1,NREC
              IF (I .EQ. NS(NN))   THEN
                OPEN(UNIT=55,FILE=SPEC(NN),FORM='UNFORMATTED')
                WRITE(55) TITLE
                WRITE(55) NT,NW,NDIM
                WRITE(55) (THETA(II),II=1,NT)
                WRITE(55) (WS(J),J=1,NW)
**
                DO II = 1,NT
                  WRITE(55) (F(II,J),J=1,NW)
                END DO
```

58

```
            CLOSE(UNIT = 55)
          END IF
        END DO
        RETURN
**
        ENTRY PLOT_FILE
        NDIM = 1
**
        OPEN(UNIT=50,FILE='surf.elv',FORM='UNFORMATTED')
        WRITE(50) TITLE
        WRITE(50) NX,NY,NDIM
        WRITE(50) (XX(J),J=1,NX)
        WRITE(50) (YY(II),II=1,NY)
**
        DO J = 1,NX
          WRITE(50) (ZETA(J,II),II=1,NY)
        END DO
        CLOSE(UNIT = 50)
**
        OPEN(UNIT=50,FILE='surf2.elv',FORM='UNFORMATTED')
        WRITE(50) TITLE
        WRITE(50) NX,NY,NDIM
        WRITE(50) (XX(J),J=1,NX)
        WRITE(50) (YY(II),II=1,NY)
**
        DO J = 1,NX
          WRITE(50) (ZETA2(J,II),II=1,NY)
        END DO
        CLOSE(UNIT = 50)
**
        RETURN
        END
**                                                                    **
************************************************************************
**                                                                    **
        REAL FUNCTION URAND(IY)
**                                                                    **
************************************************************************
**                                                                    **
**   Urand is a uniform random number generator based on theory and   **
**     suggestions given in D.E. Knuth (1968) vol.2.  The integer IY  **
**     should be initialized to an arbitrary integer prior to the first **
**     call to URAND.  The calling program should not alter the value **
**     of IY between successive calls to URAND.  Values of URAND will **
**     be returned in the interval (0,1).                             **
**                                                                    **
************************************************************************
**                                                                    **
        SAVE IA, IC, HALFM, M2, MIC, S
**
```

59

```
      DOUBLE PRECISION HALFM
**
      DATA M2/0/,ITWO/2/
**
*****  If first entry, compute machine integer worlength.
**
      IF (M2 .EQ. 0)  THEN
        M = 1
   10   M2 = M
        M = ITWO*M2
        IF (M .GT. M2) GOTO 10
        HALFM = M2
**
*****  Compute multiplier and increment for linear congruential method.
**
        IA = 8*IDINT(HALFM*DATAN(1.0D0)/8.0D0) + 5
        IC = 2*IDINT(HALFM*(0.5D0 - DSQRT(3.0D0)/6.0D0)) + 1
        MIC = (M2 - IC) + M2
**
*****  S is the scale factor for converting to floating point.
**
        S = 0.5/HALFM
      END IF
**
*****  Compute the next random number.
**
      IY = IY*IA
**
*****  The following statement is for computers which do not allow
*****   integer overflow on addition.
**
      IF (IY .GT. MIC) IY = (IY - M2) - M2
**
      IY = IY + IC
**
*****  The following statement is for computers where the
*****   wordlength for addition is greater than for multiplication.
**
      IF (IY/2 .GT. M2) IY = (IY - M2) - M2
**
*****  The following statement is for computers where integer
*****   overflow affects the sign bit.
**
      IF (IY .LT. 0) IY = (IY + M2) + M2
      URAND = FLOAT(IY)*S
**
      RETURN
      END
**
**********************************************************************
```

```
**                                                                          **
        SUBROUTINE CLEAR_DISPLAY
**                                                                          **
****************************************************************************
**
*****   Home cursor and clear display.
**
        CHARACTER*1 ESC
        CHARACTER*4 BUFFER
**
        ESC = CHAR(27)
        BUFFER = ESC//'H'//ESC//'J'
        WRITE(*,'(A)') BUFFER(1:4)
        RETURN
        END
**
****************************************************************************
**                                                                          **
        SUBROUTINE PAUSE_SEC(ISEC)
**                                                                          **
****************************************************************************
**
*****   Pauses the program by ISEC seconds.
**
        IF (ISEC .LE. 0) RETURN
**
        WRITE(*,'(8(/),"> Type < / > to continue when ready: ",$)')
        READ(*,*) SLASH
**
        RETURN
        END
```

U237033